

1-2014

Design and Synthesis of Heterocyclic Cations for Specific DNA Recognition: From AT-Rich to Mixed-Base-Pair DNA Sequences

Yun Chai

Georgia State University, ychai@gsu.edu

Ananya Paul

Georgia State University, apaul@gsu.edu

Michael Rettig

Georgia State University

W. David Wilson

Georgia State University, wdw@gsu.edu

David Boykin

Georgia State University, dboykin@gsu.edu

Follow this and additional works at: http://scholarworks.gsu.edu/chemistry_facpub

 Part of the [Chemistry Commons](#)

Recommended Citation

Design and Synthesis of Heterocyclic Cations for Specific DNA Recognition: From AT-Rich to Mixed-Base-Pair DNA Sequences Yun Chai, Ananya Paul, Michael Rettig, W. David Wilson, and David W. Boykin *The Journal of Organic Chemistry* 2014 79 (3), 852-866
DOI: <http://dx.doi.org/10.1021/jo402599s>

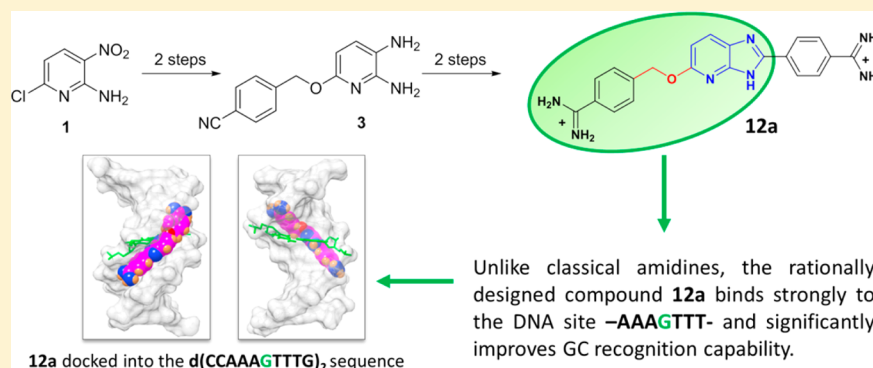
This Article is brought to you for free and open access by the Department of Chemistry at ScholarWorks @ Georgia State University. It has been accepted for inclusion in Chemistry Faculty Publications by an authorized administrator of ScholarWorks @ Georgia State University. For more information, please contact scholarworks@gsu.edu.

Design and Synthesis of Heterocyclic Cations for Specific DNA Recognition: From AT-Rich to Mixed-Base-Pair DNA Sequences

Yun Chai, Ananya Paul, Michael Rettig, W. David Wilson,* and David W. Boykin*

*Department of Chemistry, Georgia State University, Atlanta, Georgia 30303, United States

S Supporting Information



ABSTRACT: The compounds synthesized in this research were designed with the goal of establishing a new paradigm for mixed-base-pair DNA sequence-specific recognition. The design scheme starts with a cell-permeable heterocyclic cation that binds to AT base pair sites in the DNA minor groove. Modifications were introduced in the original compound to include an H-bond accepting group to specifically recognize the G-NH that projects into the minor groove. Therefore, a series of heterocyclic cations substituted with an azabenzimidazole ring has been designed and synthesized for mixed-base-pair DNA recognition. The most successful compound, **12a**, had an azabenzimidazole to recognize G and additional modifications for general minor groove interactions. It binds to the DNA site **-AAAGTTT-** more strongly than the **-AAATTT-** site without GC and indicates the design success. Structural modifications of **12a** generally weakened binding. The interactions of the new compound with a variety of DNA sequences with and without GC base pairs were evaluated by thermal melting analysis, circular dichroism, fluorescence emission spectroscopy, surface plasmon resonance, and molecular modeling.

INTRODUCTION

A serious barrier to the development of methods for rational control of gene expression in cells is the lack of a variety of small molecules that can bind strongly, for example, with nM K_D values, and sequence specifically to a range of DNA sequences.¹ Such agents have enormous potential applications in biotechnology and therapeutic development.^{2–10} With the explosion of genomic information on both sequences and their functions from bacteria to humans, the potential applications expand daily.^{11–13}

A variety of agents are needed because of variations in cell uptake potential of different molecule structures as well as pharmacokinetic differences. Surprisingly, only DNA minor groove binding polyamides, based on the natural products netropsin and distamycin, have been developed for designed recognition of a variety of DNA sequences.^{6–10} Although polyamides are now entering animal studies, none have yet gone into clinical trials.^{9,10}

Our approach to overcome the barrier to external control of gene expression by small molecules starts from an extensive library of heterocyclic cations that have AT specific binding in the DNA minor groove.^{2,4,14,15} A compound from this library has entered clinical trials, and others are clinical candidates.^{4,16–18}

Given the excellent biological activities and uptake of these compounds, we began to consider whether it might be possible to design modifications of these compounds to give them DNA sequence-specific recognition abilities.^{14,15,19,20} The key difference in DNA sequence that could make this possible is the third H-bond in GC base pairs that is not present in AT base pairs. Numerous crystal structures by the Neidle laboratory have shown that the AT-specific compounds slide deeply into the minor groove and have H-bond donating groups, such as benzimidazole and amidine-NHs, that can form strong H-bonds to the AN3 and T=O at the edges of AT base pairs in the minor groove.^{4,15,21–23} The extra H-bond in GC base pairs creates a steric barrier at the floor of the groove that prevents formation of similar complexes in an AT sequence that contains one or more GC base pairs.^{4,15,22} In polyamides, GC recognition can be designed into the structure by conversion of a pyrrole, with a **-CH** at the floor of the groove, to an imidazole, with an **-N-** in the same position, to accept an H-bond for the G-NH that projects into the groove.^{5–10,24,25}

Received: November 22, 2013

Published: January 14, 2014

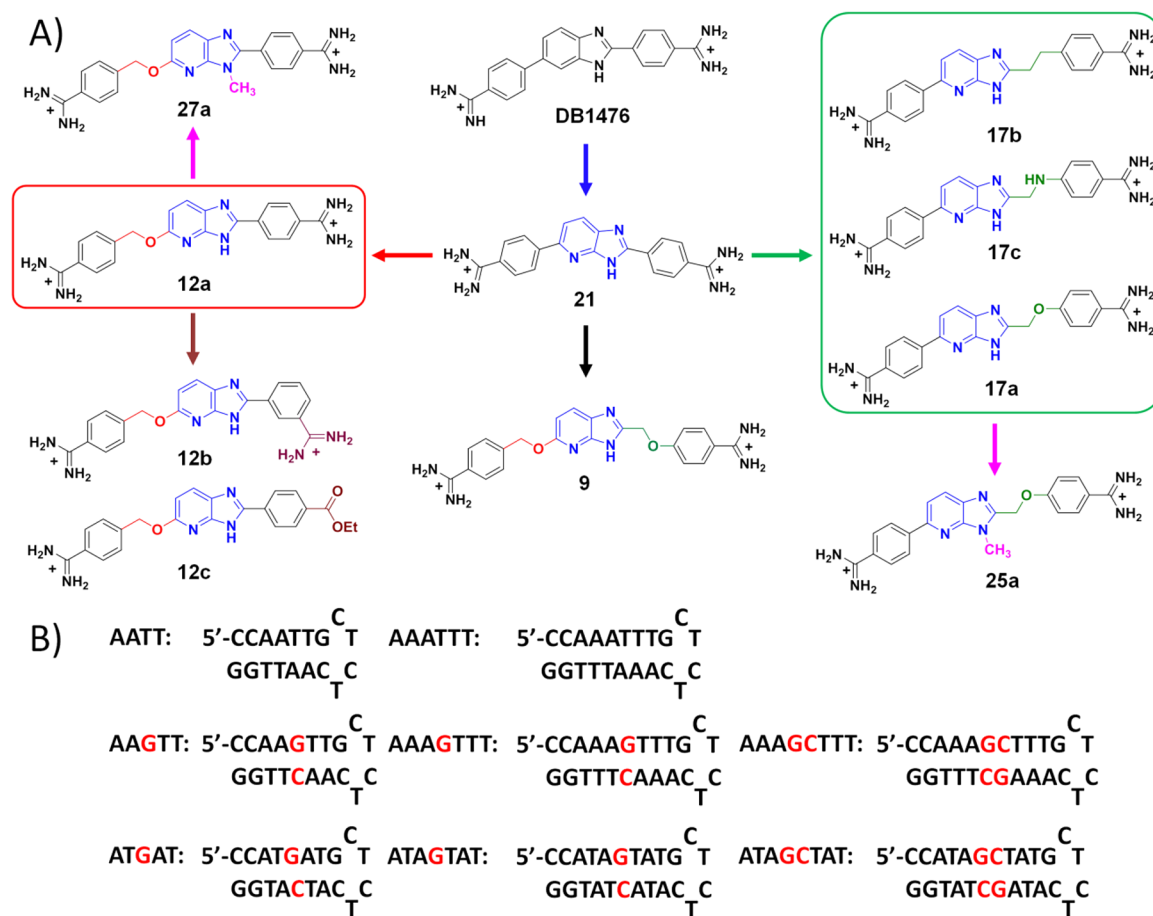
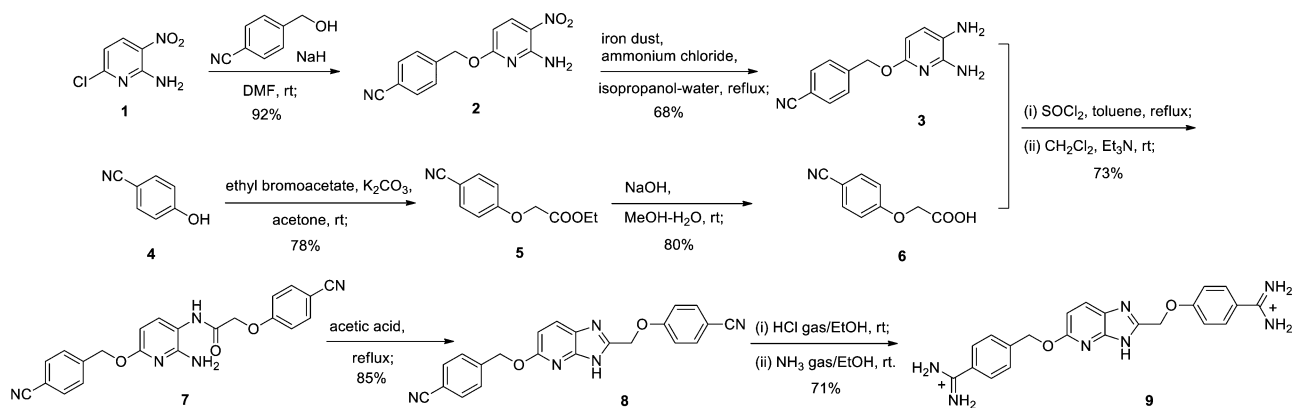


Figure 1. (A) Representative structures of compounds synthesized in this study and classified by the structural similarity. Syntheses for all new compounds are shown in Schemes 1–5. (B) Full hairpin DNA sequences are shown with the abbreviations.

Scheme 1. Synthesis of Compound 9



In the research reported here, we start with a benzimidazole-based AT-specific library compound, DB1476 (Figure 1), and convert the benzimidazole to an azabenzimidazole to evaluate enhancement in GC recognition.^{26–28} The initial compound, **21** (Figure 1) has significantly improved GC recognition capability and forms the basis for the design and synthesis of a related set of compounds for a structure-binding study. The compounds cover a broad range of chemical properties and space. **12a** (Figure 1), the best compound of this set, has significant GC recognition capability with strong binding.

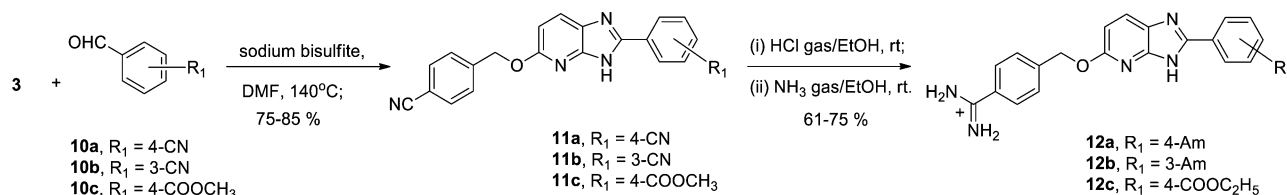
In this paper, we evaluate the relative affinities of the synthesized members of this compound set by thermal melting

analysis, the binding mode by circular dichroism, the binding affinity and stoichiometry by surface plasmon resonance, and we propose a model to explain the GC specificity by molecular modeling. The results of this study are very encouraging and show that rational design of exciting new minor groove binding structures with enhanced sequence recognition capability is possible.

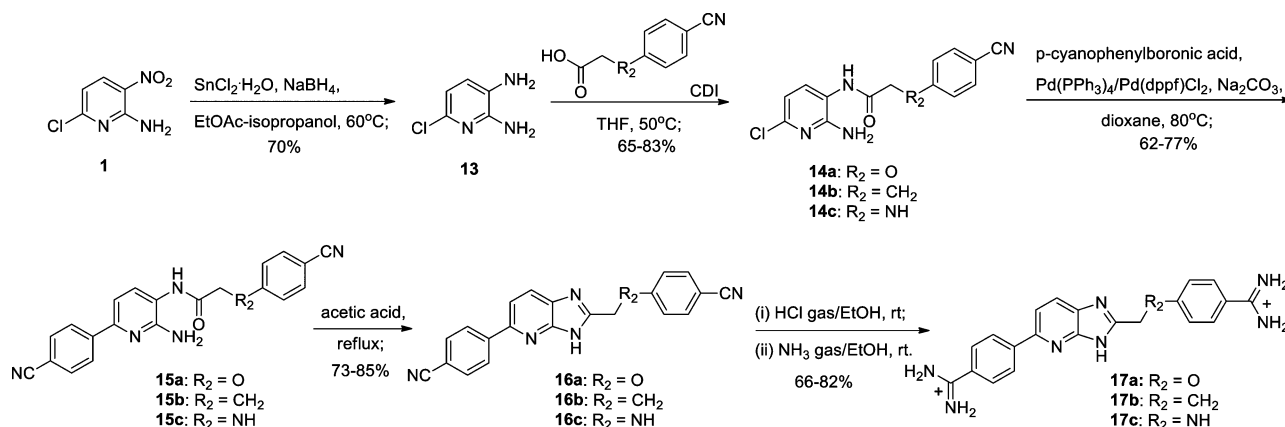
RESULTS AND DISCUSSION

Chemistry. Scheme 1 outlines our approach to synthesis of the hydrochloride salt of the azabenzimidazole diamidine **9**. 2-Amino-6-chloro-3-nitropyridine (**1**) was allowed to react with 4-

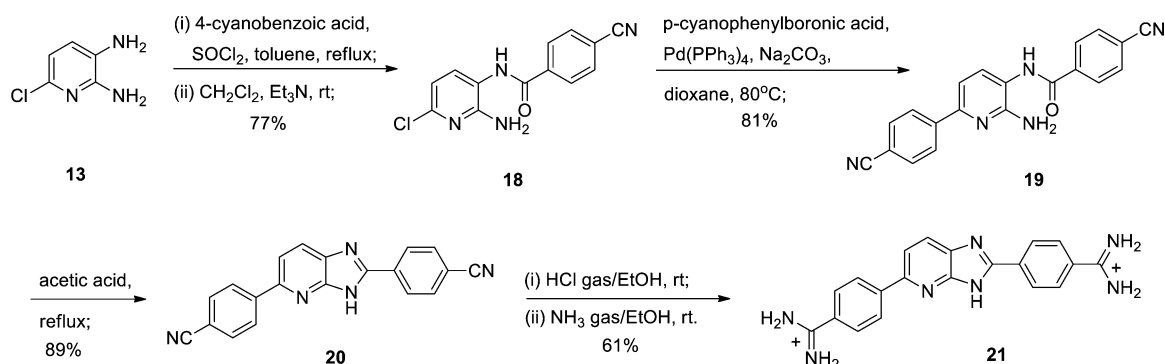
Scheme 2. Synthesis of Compounds 12a–c



Scheme 3. Synthesis of Compounds 17a–c



Scheme 4. Synthesis of Compound 21



hydroxymethylbenzonitrile in the presence of sodium hydride in dry dimethylformamide (DMF) to give compound 2. Subsequently, the reduction of the nitro group of 2 was achieved with iron dust in a 2-propanol/water mixture at reflux to produce the diamine 3.²⁹ 4-Cyanophenol (4) was reacted with ethyl bromoacetate to give the *O*-acetic acid ethyl ester 5, which was converted to acid 6 by saponification and acidification.³⁰ The acid 6 was first converted to acid chloride with thionyl chloride in dry toluene and followed by acylation with the diamine 3 to give the dinitrile 7. Cyclization of the dinitrile 7 was subsequently performed by boiling in glacial acetic acid to yield the azabenzimidazole intermediate 8.^{28,31,32} Stirring the azabenzimidazole 8 in ethanolic HCl, according to the Pinner methodology,^{33–35} afforded the bis-imidate ester hydrochloride which was then converted to the hydrochloride salt of the diamidine 9 by stirring with ethanol saturated with ammonia gas.

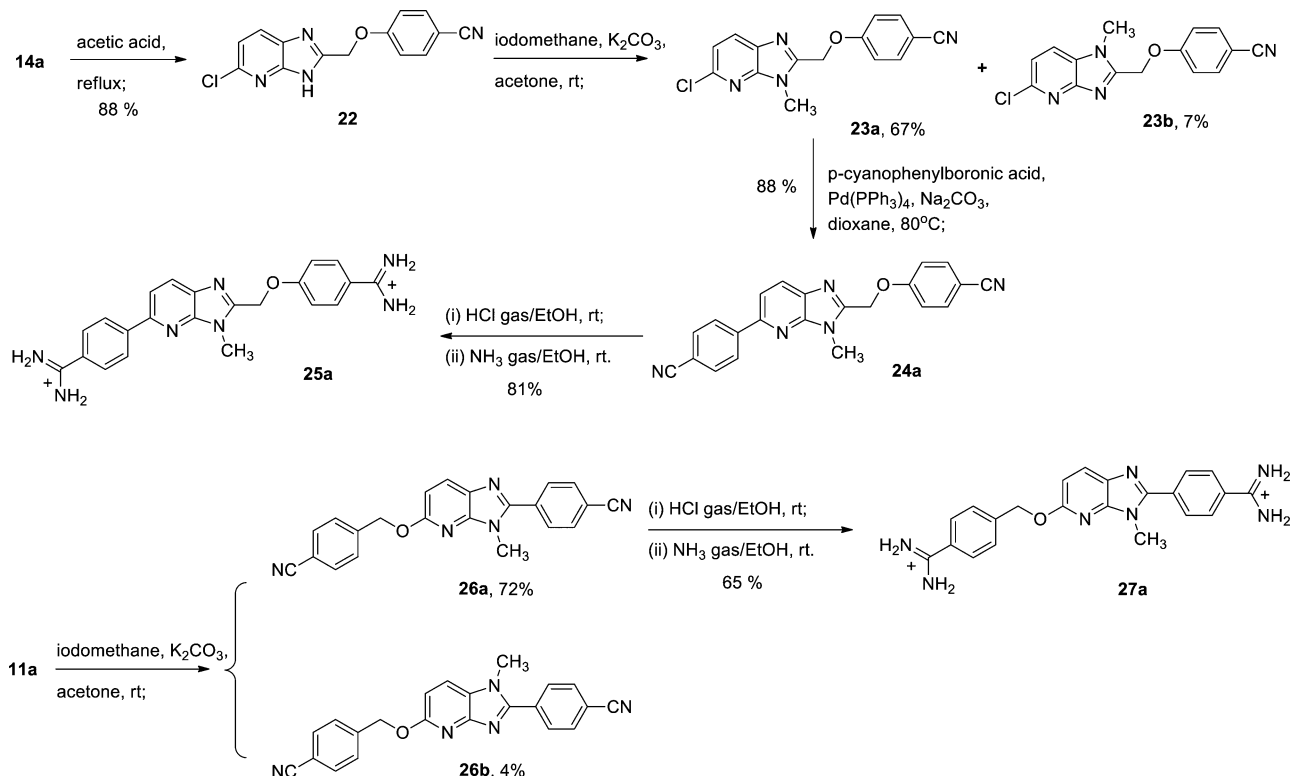
Scheme 2 illustrates the synthetic route for the three compounds 12a–c. The commercially available substituted benzaldehydes, 10a–c, were allowed to react with diamine 3 in the presence of sodium bisulfite in anhydrous DMF at reflux to afford the azabenzimidazole intermediates 11a–c.³⁶ The bis-nitrile intermediates, 11a–c, were converted to the hydro-

chloride salts of the diamidines 12a–c by applying the Pinner approach as discussed above.

Compounds 17a–c were prepared as shown in Scheme 3. 2-Amino-6-chloro-3-nitropyridine (1) was reduced to give 6-chloropyridine-2,3-diamine (13) using tin(II) chloride dihydrate and sodium borohydride in a ethyl acetate/2-propanol (9:1, v/v) mixture.³⁷ Acylation of the diamine 13 with commercially available 4-cyanophenylpropionic acid, 4-cyanophenoxyacetic acid, or 4-cyanophenylglycine in the presence of carbonyldiimidazole in dry THF gave the intermediates 14a–c.³² The dinitriles 15a–c were prepared in good yield by employing a Suzuki coupling reaction³⁸ between *p*-cyanophenylboronic acid and the chloro derivatives 14a–c using 5 mol % of Pd(PPh₃)₄/Pd(dppf)Cl₂ and 1,4-dioxane as the solvent. Cyclization of 15a–c was achieved by boiling in glacial acetic acid to yield the azabenzimidazole intermediates 16a–c, which were then converted into the diamidines 17a–c by the Pinner process.^{32,33,39}

Scheme 4 employs chemistry related to that previously described for the preparation of the diamidinoazabenzimidazole 21. 4-Cyanobenzoic acid was first converted to its acid chloride which was allowed to react with the diamine 13 to give

Scheme 5. Synthesis of Compounds 25a and 27a



compound **18**. A Suzuki coupling reaction,³⁸ similar to above, between **18** and *p*-cyanophenylboronic acid gave the dinitrile **19**. Ring closure of the dinitrile **19** with glacial acetic acid afforded the azabenzimidazole dinitrile **20**. Again, Pinner methodology was used to obtain the diamidine **21**.

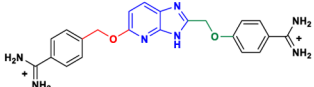
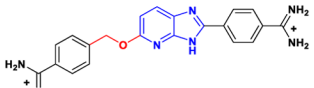
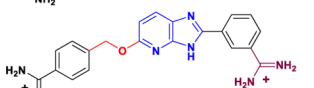
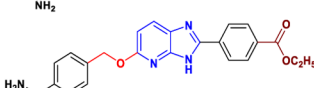
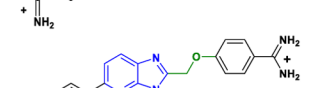
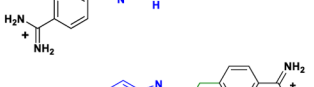
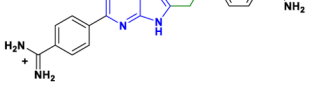
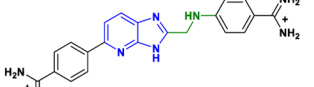
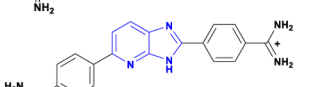
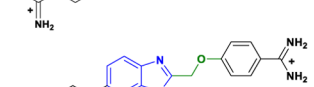
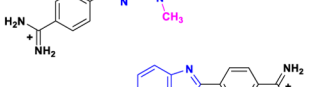
Scheme 5 illustrates the synthesis of compounds **25a** and **27a**, which are *N*-methyl analogues of **17a** and **12a**, respectively. After cyclization of compound **14a** in acetic acid, the resulting derivative **22** was methylated using methyl iodide in acetone in the presence of potassium carbonate, which gave a mixture of isomers **23a** and **23b**. The isomers were separated by column chromatography on silica gel in 67% and 7% isolated yields, respectively. A Suzuki coupling reaction, then the Pinner process was applied to **23a** to obtain the diamidine **25a**. Compound **27a** was prepared using a similar sequence of reactions starting from **11a**.

Thermal Melting (T_m): Ranking of Relative DNA Complex Stabilities. Thermal melting experiments allow a rapid and robust screening for the relative binding affinity and the sequence selectivity of the ligands with the different DNA sequences (Table 1).^{40,41} In general, the DNA melting transition is characterized by a single cooperative absorbance change as a function of temperature. Compound binding to the DNA is expected to enhance the duplex stability when compared to single strands, and an increase in the DNA melting temperature upon drug addition is therefore associated with its relative binding affinity.⁴² DNA AT sequences with zero, one, or two GC base pairs (Figure 1) were used as targets for the designed compounds, and the results are summarized in Table 1. The melting profiles are shown in the Supporting Information (Figure S1). The parent benzimidazole core diamidine, DB1476, is a reference compound and binds strongly with pure AT-rich sequences (AATT $\Delta T_m = 11.3$ °C and AAATTT $\Delta T_m = 17.2$ °C, in Table 1), but it has a weak affinity toward the mixed DNA

sequences which are separated by a single or two GC base pairs (AAGTT $\Delta T_m = 4.8$ °C, AAAGTTT $\Delta T_m = 9.3$ °C, and AAAGCTTT $\Delta T_m = 6.2$ °C). Compound **21** with the substitution of the benzimidazole core with an azabenzimidazole showed decreased thermal stabilities with the pure AT rich sequences (AATT $\Delta T_m = 4.5$ °C and AAATTT $\Delta T_m = 8.1$ °C) and slightly increased thermal stabilities with mixed DNA sequences AAGTT and AAAGTTT ($\Delta T_m = 8.6$ and 9.2 °C, respectively).

The crucial breakthrough in developing strong and selective GC base pair recognition was achieved with the linker $-\text{CH}_2\text{O}-$ being inserted between the azabenzimidazole and phenyl of **21** to yield **12a**. In an effort to improve the G-recognition of **21**, we considered introduction of flexible linkers between the phenyl-amidine and the azabenzimidazole. To maintain curvature to match the minor groove a two atom linker is required and we opted to use a $-\text{CH}_2\text{O}-$ linker, as opposed a $-\text{CH}_2\text{CH}_2-$ one, based on modeling studies (not shown). The studies suggest that the presence of an $-\text{O}-$ versus $-\text{CH}_2-$ allows greater flexibility for groove-binding and possibly reduces steric hindrance to the approach of $\text{N}-\text{H}$ to the pyridine nitrogen. This hypothesis needs to be tested by synthesis of the $-\text{CH}_2\text{CH}_2-$ analogue of **12a** which is a part of ongoing studies. Introducing the $-\text{CH}_2\text{O}-$ linker resulted in a pronounced increase in the thermal stability of the single GC containing AAGTT ($\Delta T_m = 13.3$ °C) and AAAGTTT ($\Delta T_m = 15.3$ °C, Table 1) sequences. Compound **12a** also showed sequence selectivity with relatively weak binding to the pure AT sequences (AATT $\Delta T_m = 6.1$ °C and AAATTT $\Delta T_m = 12.4$ °C). The ΔT_m values of **12a** with AAGTT and ATGAT sequences are 13.3 and 4.8 °C, while AAAGTTT and ATAGTAT sequences are 15.3 and 9.4 °C. This suggests more favorable interactions within the narrow grooves of pure A-tract DNAs relative to the wider groove in alternating AT sequence DNAs.^{12,43,44} Introducing the $-\text{CH}_2\text{O}-$ linker clearly increases

Table 1. Thermal Melting Studies (ΔT_m ,^a °C) of the Designed Heterocyclic Amidine Compounds with Mixed DNA Sequences

Compound	Structure	AAAGTT	ATGAT	AAIT	AAAAGTTT	ATAGTAT	AAATTT	AAAAGCTTT	ATAGCTAT
9		3.2	1.6	<1.0	6.2	2.0	2.5	2.8	<1.0
12a		13.3	4.8	6.1	15.3	9.4	12.4	6.6	4.2
12b		5.5	1.9	3.4	6.3	2.2	4.6	1.7	<1.0
12c		4.3	1.3	1.7	4.5	3.2	2.2	2.3	1.2
17a		2.6	1.4	1.3	3.9	1.6	1.3	1.7	1.1
17b		1.4	<1.0	1.1	2.4	1.3	1.5	1.3	<1.0
17c		2.2	<1.0	1.0	2.1	<1.0	3.6	3.6	<1.0
21		8.6	4.0	4.5	9.2	3.8	8.1	3.2	2.5
25a		<1.0	<1.0	1.2	<1.0	<1.0	2.5	<1.0	<1.0
27a		2.8	1.1	1.8	4.0	1.4	3.1	1.0	1.0
DB1476		4.8	3.8	11.3	9.3	6.5	17.2	6.2	4.2

^a: $\Delta T_m = T_m(\text{the complex}) - T_m(\text{the free DNA})$. The listed values are for 2:1 [ligand]/[DNA] ratio and an average of two independent experiments with a reproducibility of ± 0.5 °C.

the conformational mobility of **12a** and also opens up the space for the azabenzimidazole core for the G recognition. Interestingly, **12a** did not show any enhancement in thermal stabilities for two GC containing sequences (Table 1).

Surprisingly, the structural isomer of **12a**, **17a** with the $-\text{OCH}_2-$ linker attached at the 2-position of the azabenzimidazole core, resulted in a large decrease of the thermal stability of all the eight tested DNA sequences (ΔT_m 1.1–3.9 °C). Similar weaker thermal stability results relative to **12a** were observed when the $-\text{OCH}_2-$ linker was replaced with $-\text{CH}_2\text{CH}_2-$ (**17b**) or $-\text{NHCH}_2-$ (**17c**). Also for **9**, with the $-\text{OCH}_2-$ linker

attached at the 2-position of the azabenzimidazole core for **12a**, only moderate DNA binding for a single GC base pair sequences (AAAGTTT $\Delta T_m = 6.2$ °C) was observed. These results indicate that the rigidity of the amidinium–phenyl–azabenzimidazole system and the unfavorable twist of the linker–phenyl–amidinium in part account for the weak binding. The replacement of the 4-amidinium with 3-amidinium group (**12b**) yields a tighter curvature and did not result in any increase in ΔT_m compared to **12a**. The amidinium to $-\text{COOEt}$ change (**12c**), as expected, resulted in a major decrease in the thermal stability of all the tested DNA sequences. This

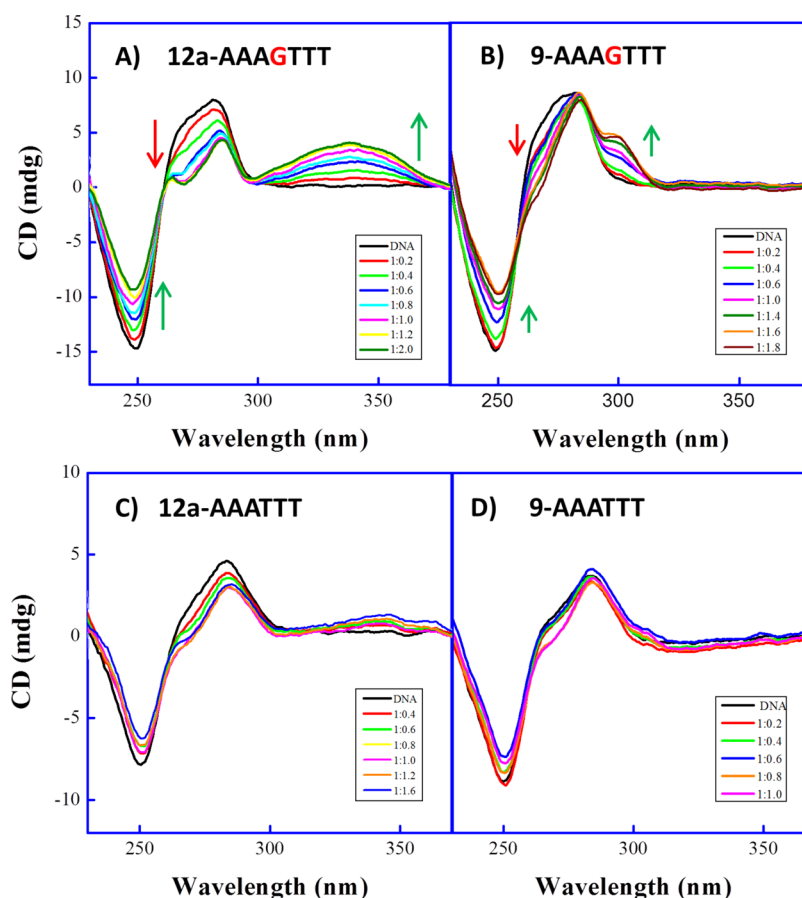


Figure 2. Circular dichroism spectra of representative compounds, **12a** and **9**, with the AAAGTTT and AAATTT DNA sequences. (A) The ratios of **12a** to AAAGTTT from the bottom to the top are 0, 0.2, 0.4, 0.6, 0.8, 1.0, 1.2, 2.0. (B) The ratios of **9** to AAAGTTT are 0, 0.2, 0.4, 0.6, 1.0, 1.4, 1.6, 1.8. (C) The ratios of **12a** to AAATTT are 0, 0.4, 0.6, 0.8, 1.0, 1.2, 1.6. (D) The ratios of **9** to AAATTT are 0, 0.2, 0.4, 0.6, 0.8, 1.0. Color arrows indicate positive (green) and negative (red) induced changes. The experiments were conducted in Tris-HCl buffer at 25 °C.

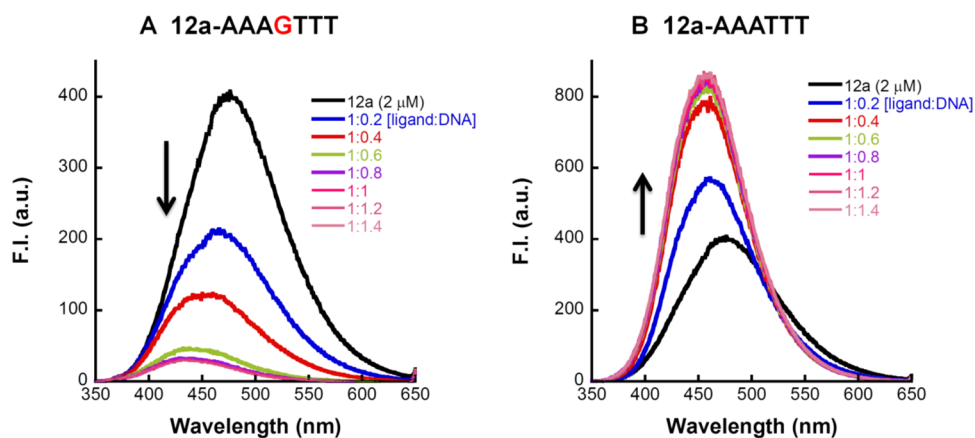


Figure 3. Fluorescence emission spectra for **12a** titrated with AAAGTTT (A) and **12a** titrated with AAATTT: 2 μM solution of **12a** in 10 mM Tris-HCl, 100 mM NaCl, pH 7.4 buffer at 25 °C. Each addition of hairpin DNA resulted in an increase of DNA concentration of 0.4 μM . Arrows indicate induced changes in fluorescence. Under these concentration conditions **12a** is fully bound to the DNA at the highest concentrations shown in the Figures.

demonstrates that a dication with specific curvature is needed for optimizing minor groove binding. **25a** and **27a**, *N*-methyl analogues of **17a** and **12a**, resulted in significant decreases in ΔT_m values due to steric effects and lack of H-bonding interactions with the G-NH₂ group. All the compounds of this series showed very weak binding to two GC base pair containing DNA sequences.

Circular Dichroism (CD): Probing the Binding Mode. Circular dichroism spectroscopy is a valuable technique for characterizing DNA minor groove interactions.⁴⁵ CD titration experiments as a function of compound concentration were performed to monitor the induced CD, the binding mode and the saturation limit for selected compounds (**12a** and **9**) binding with the AAAGTTT and AAATTT sequences (Figure 2).

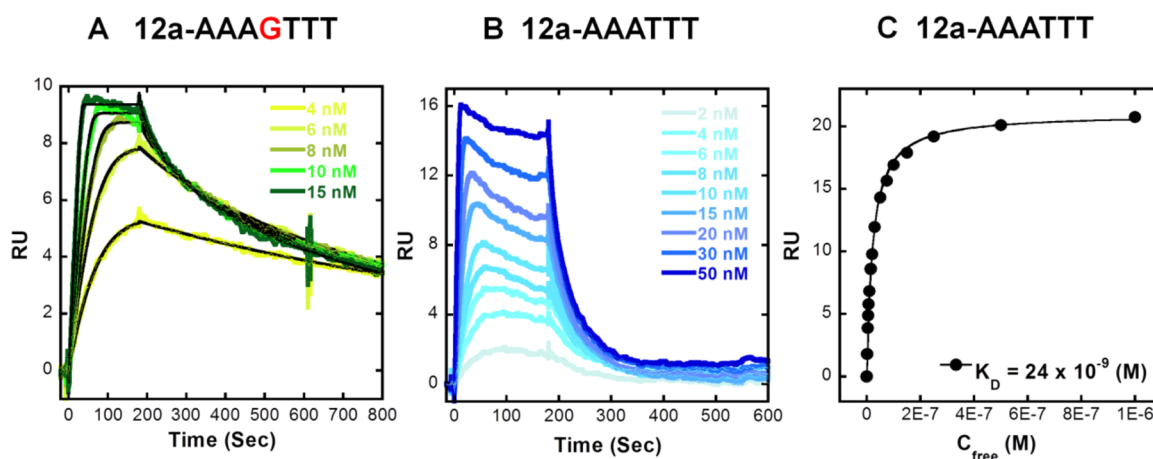


Figure 4. Representative SPR sensorgrams for **12a** in the presence of (A) AAAGTT and (B) AAATTT hairpin DNAs. In (A) the solid black lines are best fit values for global kinetic fitting of the results with a single site function. (C) Binding plots for AAATTT with **12a** and the data was fitted to a steady-state binding function using a 1:1 model to determine equilibrium binding constants.

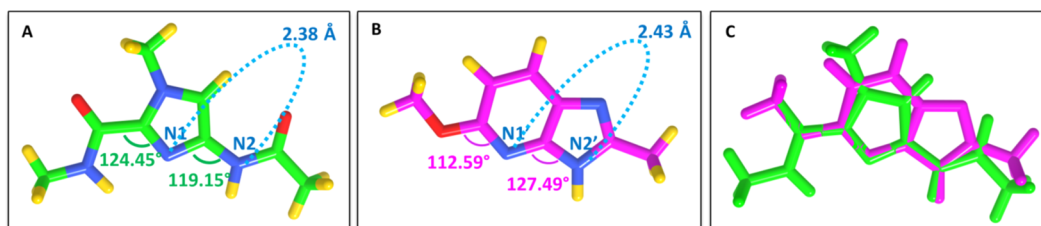


Figure 5. Design concept of azabenzimidazole-containing heterocyclic diamidines for mixed sequence DNA recognition. Energy minimized structure and the structural properties of (A) the imidazole motif used in synthetic polyamides that recognizes a G base in a GC base pair and (B) an azabenzimidazole motif (Spartan 10 software). The angles and distances are shown as arc line and blue dashed line with numbers. (C) The alignment of the imidazole motif (in green color) and azabenzimidazole motif (in pink color) units using Sybyl1.2 software. The images were drawn with the UCSF Chimera Software.

Neither the hairpin DNA nor the free compound exhibits CD signals in the compound absorption region above 300 nm. Addition of minor groove binders to DNA results in substantial positive induced CD signals on complex formation with DNA at the wavelengths between 300 and 400 nm.

Figure 2A,C show the CD spectra of **12a** with the AAAGTTT and AAATTT sequences, respectively. Upon addition of **12a** to the AAAGTTT sequence, the expected strong positive CD signals in the compound absorption region (300 to 380 nm) are indicative of a minor groove binding mode, with relatively small and consistent changes in the DNA CD spectral region (Figure 2A). It seems likely that the shape of **12a** does not exactly match the free DNA minor groove shape. In this case, the compound induces complementary changes in the DNA structure, and the CD spectral region, which yield a very favorable final complex with a high T_m value. In addition, **12a** gives significant induced CD signals with saturation near a 1:1 compound to DNA ratio, which suggests **12a** binds as a monomer in the minor groove of the AAAGTTT sequence (Supporting Information, Figure S2). On the other hand, **12a** shows a very weak ICD for the AAATTT sequence, indicating it has much stronger sequence specificity toward the mixed DNA sequence than pure AT rich sites as observed in T_m experiments.

Compound **9** shows moderate ICD enhancement with the AAAGTTT sequence (Figure 2B). Small and consistent changes in the CD spectral region of DNA (230 to 290 nm) are observed with incremental titration of ligands indicating only minor conformational changes in DNA on complex formation. However, in the presence of a pure AT sequence (Figure 2D)

no ICDs are observed, in agreement with the T_m results. Compound **17a** and the other analogues show very weak binding for both AAAGTTT and AAATTT DNAs (Supporting Information, Figure S3).

Fluorescence Emission Spectroscopy. Fluorescence emission spectroscopy changes on binding are very informative for the lead compound **12a**. Titrations of **12a** with AAAGTTT and AAATTT sequences are shown in Figure 3, and the compound has very different induced spectral changes on complex formation with these two DNA sequences. The fluorescence intensity of **12a** quenched on addition of the AAAGTTT sequence and slightly increased upon binding to the AAATTT sequence. The fluorescence quenching by a G base is a well established phenomenon.^{46–48} The results suggest that **12a** can interact with both sequences and are in agreement with the T_m and CD results. Under the conditions of the fluorescence experiments, **12a** is essentially fully bound to the DNAs at a 1:1 ratio.

Biosensor Surface Plasmon Resonance (SPR): Determining Binding Affinity and Stoichiometry. Biosensor SPR methods provide an excellent way to quantitatively evaluate the interaction of small molecules with DNA and other biomolecules.^{49–51} Because the SPR approach responds to mass, it is an excellent method for comparative studies of dications that have very large differences in properties and equilibrium binding constants, K . Because it responds to mass, the signal at saturation of binding sites directly provides the stoichiometry. SPR sensorgrams were collected (Figure 4A,B) and were subjected to steady-state analyses.^{49–51} The sensorgrams were fitted to appropriate

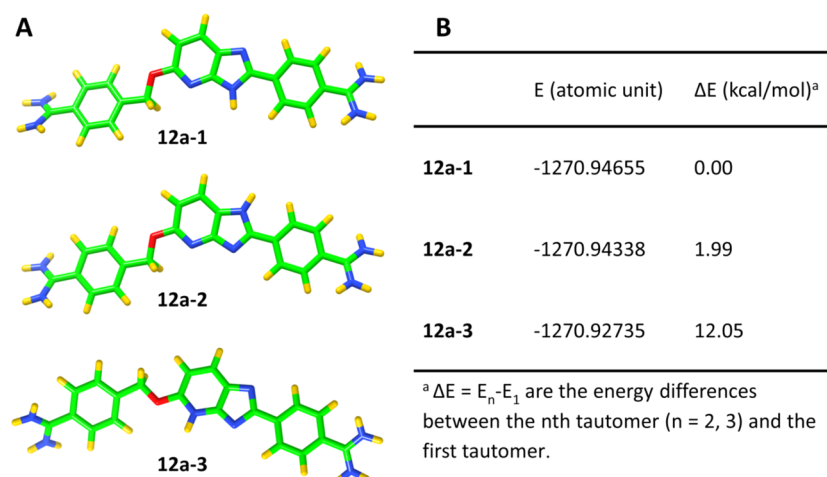


Figure 6. (A) Equilibrium geometry of three possible tautomeric forms of **12a** calculated by density functional theory (DFT/B3LYP) with the 6-31G* polarization basis set. (B) The table on the right displays the calculated total energies E (atomic unit) and relative ΔE (kcal/mol) energies of **12a** tautomers.

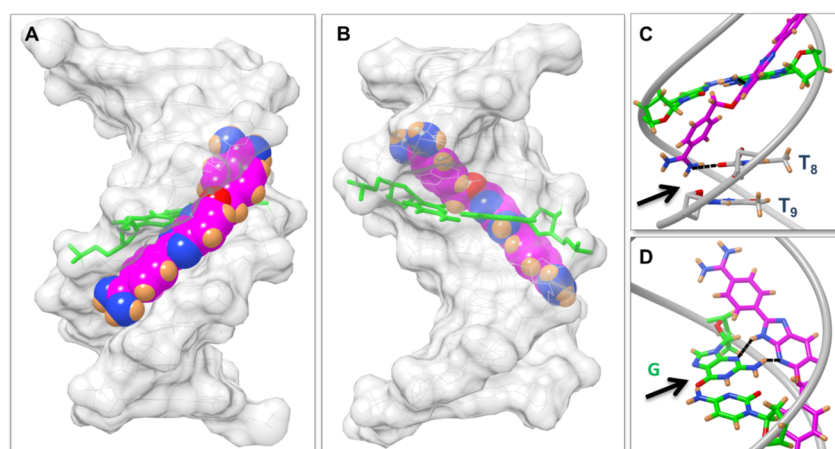


Figure 7. Molecular models for **12a** docked into the d(CCAAAGTTTG)₂ sequence. The images are of only the lowest-energy conformation and have been drawn with the UCSF Chimera Software. View from (A) minor and (B) major groove, the solvent accessible surface is shown as light gray with 70% transparency to heighten clarity, the GC base pair is in green with **12a** in magenta. Note close contact of the surfaces of **12a** with the DNA minor groove wall surfaces. (C) Detailed views from the minor groove of the hydrogen-bond interactions between one amidinium group of **12a** and the O2 atom of thymine 8 (black dashed line). (D) Detailed views from major groove of the hydrogen-bond interactions between the inner-facing azabenzimidazole -N- and -NH atoms with G NH₂ and G N3 groups of **12a** (black dashed line).

binding models to determine K values (Experimental Section). On the basis of T_m and CD studies, compound **12a** was selected for SPR binding studies.

As can be seen in Figure 4A, compound **12a** binds strongly with the single GC base-pair sequence, AAAGTTT ($K_D = 0.3 \times 10^{-9}$ M), as a monomer. The strong binding observed with this compound can be attributed to the rapid association and the slow dissociation rates (Figure 4A). However, the binding affinity of **12a** with pure AAATTT is significantly lower, $K_D = 24 \times 10^{-9}$ M, which is 80 fold weaker than the single GC binding (Figure 4B,C). These results also indicate that the compound **12a** has strong sequence selectivity toward single GC mixed sequences. This supports results from T_m and CD studies.

Molecular Modeling Studies: Visualization of 12a-AAAGTTT Complex. To better understand the binding of **12a** with the AAAGTTT sequence, it is informative to compare structural similarities between the azabenzimidazole core of **12a** and the imidazole group of polyamides.^{52,53} Density functional theory (DFT) calculations for optimizing geometry for the azabenzimidazole core and the imidazole-containing amides are

shown in Figure 5A and 5B, and the alignment of their structural skeletons is shown in Figure 5C to clarify the similarity of these two units. The inner faces of these two molecules, which face the floor of the minor groove, have very similar character and can form hydrogen bond interactions with GC base pairs. These comparisons illustrate the ability of **12a** to recognize a G base in a similar manner to imidazole.^{52,26}

Since a 2,5-substituted azabenzimidazole ring has three possible tautomeric forms, **12a** was taken as an example for tautomer energy analysis (Figure 6). Geometry-optimized models for **12a** tautomers are shown in Figure 6A, and the calculated single-point energy predictions are compared in Figure 6B. The results show that **12a-1** has the lowest energy value among the three tautomers. The methylation results of **11a** (in Scheme 5) are consistent with the theoretical calculation results. We thus used the tautomer where the hydrogen is on the 3-position of the benzimidazole ring for the following docking studies.

To provide ideas for a better understanding of the observed strong binding affinity of **12a**, it was docked as a monomer into

the central –AAAGTTT– site of the minor groove of the 5'-d(CCAAAGTTTG)-3' duplex (Figure 7A,B). As can be seen, this model predicts that **12a** closely matches the minor groove shape, and the azabenzimidazole module is oriented parallel to the groove walls in the model in Figure 7. This orientation provides excellent groove recognition units for both GC (azabenzimidazole) and AT (phenyl-amidine) base pairs. The model also predicts that the amidinium group, attached to the phenyl-CH₂O- group, is involved in hydrogen bonding to the O2 atom of thymine 8 (2.4 Å, Figure 7C), while the inner-facing azabenzimidazole –N– and –NH atoms are involved in hydrogen bonding to the G NH₂ and G N3 groups (2.7 and 2.8 Å, respectively, Figure 7D). The other amidinium group does not directly participate in hydrogen bonding with the DNA but is close to the mouth of the minor groove and in close proximity to DNA phosphates for favorable electrostatic interaction, but further optimization of the compound for minor groove H-bonding should be possible.

CONCLUSIONS

Design of compounds for recognition of the mixed DNA sequences has been successfully achieved with minor groove binding polyamides. While much has been learned from the studies of a variety of polyamides, effective, specific therapeutic targeting of DNA would greatly benefit from the availability of additional sequence-specific molecules. The primary goal of this project takes advantage of the widely known AT preferences of many minor groove binders by incorporating an azabenzimidazole ring in such a way as to create a motif for GC base-pair recognition. The data presented in this report indicate that this series of heterocyclic cations have different DNA binding properties, which are highly dependent on the structure of compounds and also on the DNA sequences.

Starting with a classical type, AT-specific minor groove binding compound, DB1476, the structure was significantly modified to introduce GC recognition. The design, synthesis, and DNA interaction studies were successful in producing **12a**. Compound **12a** is the first designed, nonpolyamide compound that is capable of selective recognition of sequences with a single GC base pair in an AT sequence context. It is an important breakthrough in the rational design of DNA sequence-specific binding compounds. Molecular modeling has clearly demonstrated the effective interactions of **12a** with a G base. Removal of the GC base pair or addition of another GC significantly weakens DNA binding of **12a** relative to the single G sequence. Isomers and modifications of **12a** also reduced specific GC base pair recognition.

The results presented here clearly show that rational design of nonpolyamide compounds for binding to mixed DNA sequences is possible and can potentially produce agents for selective inhibition of DNA–protein complexes such as transcription factor (TF) complexes. TFs have been classified as “undrugable” biopolymers for direct inhibition and the approach represented here suggests a different inhibition route. The success of **12a** with mixed DNA sequence recognition capability offers important insights and exciting new information that can be integrated into future compound design efforts and finally in expanding the DNA targeting field.

EXPERIMENTAL SECTION

DNA Oligonucleotides. For the thermal melting, circular dichroism, and fluorescence emission spectroscopy experiments, hairpin DNA oligomers used were AAGTT [5'-CCAAAGTTGCTCTCAACTTGG-3'], ATGAT [5'-CCATGATGCTCTCATCATGG-3'], AATT

[5'-GCCAATTGCCTCTGC AATTGGC-3'], AAAGTTT [5'-CCAAAGTTTGCCTCTCAACTTTGG-3'], ATAGTAT [5'-CCATAGTATGCTCTCATACTATGG-3'], AAATTT [5'-CCAAATTTGCCTCTGCAAATTTGG-3'], AAAGCTTT [5'-CCAAAGCTTTGCTCTCAAAGCTTTGG-3'] and ATAGCTAT [5'-CCATAGCTATGCTCTCATAGCTATGG-3'] with the hairpin loop sequences underlined (Figure 1). Lyophilized DNA oligomers were purchased from Integrated DNA Technologies, Inc., via HPLC purification. Doubly distilled water was added to the solid DNAs to bring the concentration to approximately 1.0 mM, based on the reported amount of DNA from IDT. The molar concentrations of these hairpin DNAs were then determined using a UV–vis spectrophotometer at 260 nm based on the molar extinction coefficients (ϵ_{260}) calculated by the nearest neighbor method.

Thermal Melting (T_m). Thermal melting experiments were performed on a UV–vis spectrophotometer. The concentration of each hairpin DNA sequence was 3 μ M, and experiments were in buffer (50 mM Tris–HCl, 100 mM NaCl, 1 mM EDTA, pH 7.4) in 1 cm quartz cuvettes at various ligand–DNA ratios [0:0 (buffer blank), 0:1 (DNA only, as a control), 1:1 and 2:1]. The DNA solutions were annealed prior to being tested. The spectrophotometer was set at 260 nm, 0.5 °C/min increase beginning at 25 °C, well below the DNA melting temperature and ending well above it or at 95.00 °C. The absorbance of the buffer was subtracted, and a graph of normalized absorbance vs. temperature was created using Kaleidagraph software. The ΔT_m values were calculated using a combination of the derivative function and estimation from the normalized graphs.

Circular Dichroism Spectroscopy (CD). Circular dichroism experiments were performed on a CD spectrometer in 1 cm quartz cell at 25 °C. The hairpin DNA (5 μ M) sequence in buffer (50 mM Tris–HCl, 100 mM NaCl, 1 mM EDTA, pH 7.4) was added to the cell prior to the experiment and then the compound was added to the hairpin DNA solution and incubated for 10 min to achieve the equilibrium binding for the DNA complex. For each titration point four spectra were averaged from 500 to 220 nm with scan speed 50 nm/min, and a response time of 1 s. Buffer subtracted graphs were created using the Kaleidagraph software.

Fluorescence Emission Spectroscopy. Fluorescence spectra were recorded on a Bio Spectrofluorimeter, with excitation and emission slit width fixed at 5 nm. The free compound solution at concentration of 2 μ M was prepared in buffer (10 mM Tris–HCl, 100 mM NaCl, pH 7.4), and DNA aliquots were added from a concentrated stock. The spectra were collected after allowing an equilibration time of 10 min. **12a** was excited at 330 nm, based on results from UV–vis spectroscopy. Emission spectra were monitored from 430 to 450 nm. All the fluorescence titrations were performed at 25 °C.

Biosensor Surface Plasmon Resonance (SPR). SPR measurements were performed with four-channel Biacore T200 and T100 optical biosensor systems. 5'-Biotin-labeled DNA sequences (AAAGTTT and AAATTT hairpins, in Figure 1) were immobilized onto streptavidin-coated sensor chips as previously described.^{49,50} The SPR experiments were performed at 25 °C in degassed and filtered Tris–HCl buffer (50 mM Tris–HCl, 100 mM NaCl, 1 mM EDTA, pH 7.4). Steady-state binding analysis was performed with multiple injections of different compound concentrations over the immobilized DNA surface at a flow rate of 100 μ L/min. Solutions of known **12a** concentrations were injected through the flow cells until a constant steady-state response was obtained. Compound solution flow was then replaced by buffer flow resulting in dissociation of the complex. After each cycle, the sensor chip surface was regenerated with a 10 mM glycine solution at pH 2.5 for 30 s followed by multiple buffer injections to yield a stable baseline for the following cycles. The reference response from the blank cell was subtracted from the response in each cell containing DNA to give a signal (RU, response units) that is directly proportional to the amount of bound compound. The predicted maximum response per bound compound in the steady-state region (RU_{max}) was determined from the DNA molecular weight, the amount of DNA on the flow cell, the compound molecular weight, and the refractive index gradient ratio of the compound and DNA, as previously described.⁵¹ RU was plotted as a function of free ligand concentration (C_{free}), and the

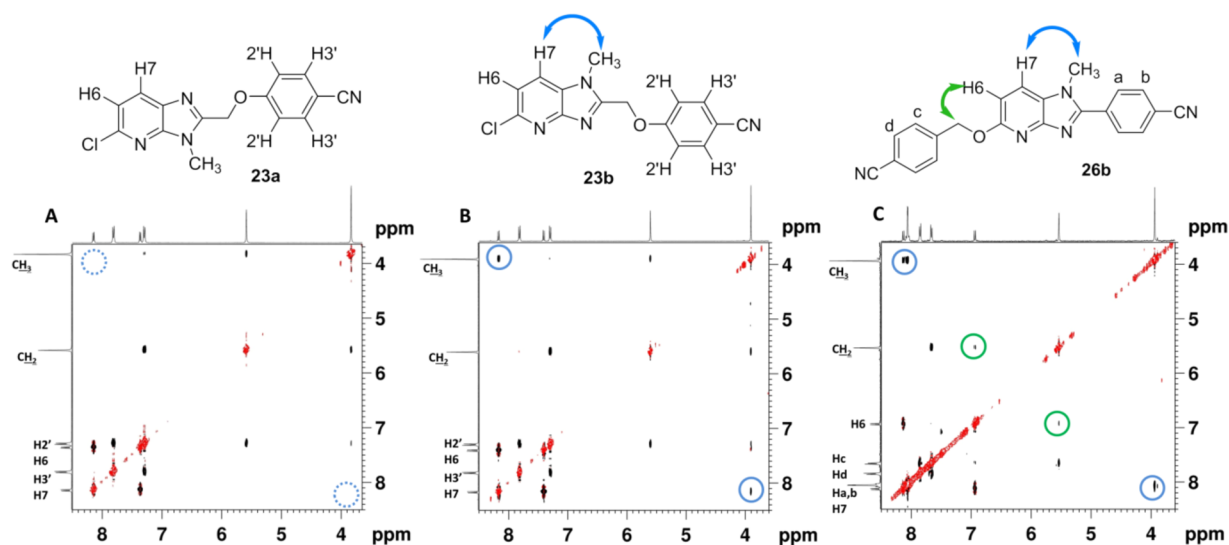


Figure 8. NOESY spectra (400 MHz, DMSO- d_6) of (A) the pure major isomer **23a** showing the lack of correlation between H7 and the methyl protons (blue dashed circle), (B) the pure minor isomer **23b** showing correlation between H7 and the methyl protons (blue solid circle), and (C) the minor isomer **26b** showing correlation between H7 and the methyl protons (blue solid circle), between H6 and the methylene protons (green solid circle).

equilibrium binding constants were determined with a one-site binding model ($K_2 = 0$).

$$r = (K_1 C_{\text{free}} + 2K_1 K_2 C_{\text{free}}^2) / (1 + K_1 C_{\text{free}} + K_1 K_2 C_{\text{free}}^2) \quad (1)$$

Where r represents the moles of bound compound per mole of DNA hairpin duplex, K_1 and K_2 are macroscopic binding constants and C_{free} is the free compound concentration in equilibrium with the complex. RU_{max} in the equation was used as a fitting parameter, and the obtained value was compared to the predicted maximal response per bound ligand to independently evaluate the stoichiometry. Kinetic analysis was performed by globally fitting the binding results for the entire concentration series using a standard 1:1 kinetic model with integrated mass transport-limited binding parameters as described previously.^{19,49–51}

Structural Model Calculation Methods. Molecular modeling studies were initiated with conformational analysis of the tested compounds with a molecular mechanics MMFF approximation level with the Spartan 10 software package. The software package was employed to optimize the final geometry by using ab initio calculations with density functional theory (DFT), B3LYP at the 631G* approximation level. The molecular energy was calculated by employing the Hartree–Fock approximation also at the 631G* level. The alignment of compounds was done using the “Align Database” option of the QSAR module in SYBYL-X1.2 software package on a windows workstation.⁵⁴

Molecular docking and visualization studies were performed with the SYBYL-X1.2 software. The initial DNA duplex 5'-d(CCAAAGTTTG)-3' was constructed in the Biopolymer-Build DNA Double Helix module employing regular B-DNA parameters. The DNA was next energy minimized for a maximum of 100 iterations using the conjugate gradient algorithm and Tripos force field, with a termination gradient of 0.1 kcal/(mol Å). The three-dimensional structure of **12a** was built, assigned Gasteiger–Hückel charges, and minimized using the Tripos force field until a terminating conjugate gradient of 0.01 kcal/mol Å or the maximum 1000 iterations was reached.^{54,19}

During the docking process, **12a** and the DNA were in separate molecular areas within the SYBYL graphical user interface. Compound **12a** was manually inserted into the DNA minor groove, and the Flexidock module was then employed. Ten different random numbers were designed and employed by the genetic algorithm, one at a time, for a total of 10 docking trials. A total of 456000 generations were calculated and assigned for docking **12a** into the DNA minor groove.^{54–56} The large amount of generations ensured that the lowest energy conformations were obtained. Both the ligand and the bound DNA

were permitted torsional flexibility in the docking process. Atomic charges were computed using Kollman all-atom for DNA and Gasteiger–Hückel for the ligands. All of the possible hydrogen-bond sites were selected for the DNA–ligand complex. From each docking, the 20 lowest energy structures were selected.

Methylation Position of Azabenzimidazole Ring. The isomers (**23a**, **23b**) were successfully isolated from the mixture by column chromatography on silica gel. In addition to mass spectrometry and $^1\text{H}/^{13}\text{C}$ NMR, two-dimensional nuclear overhauser effect spectroscopy (NOESY) NMR studies were performed. After the signals were fully assigned by a thorough interpretation of all other spectra, the NOESY spectra allowed for a detailed characterization of the isomer structures. The two NOESY spectra of the isomers are presented in Figure 8A,B. The relative intensity of the NOE crosspeaks between CH_2 and H_2' , CH_3 and CH_2 , CH_3 and H_2' , H_2' and H_3' along with H_6 and H_7 were observed in both NOE studies for the two isomers. The most important diagnostic signal, of particular interest, was the correlation of CH_3 and H_7 which is on the pyridine ring. There is a correlation that can be seen between H_7 and CH_3 of the minor isomer (blue solid circle in Figure 8B), which leads to the conclusion that the minor isomer has the stereochemistry indicated as **23b**; While no correlation is seen between H_7 and CH_3 (blue dashed circle in Figure 8A) in the major isomer, it is characterized as **23a** (Scheme 5).

Based on the results obtained for the isomer **23b**, it was found that the isomer **26b** has the same relative configuration, in which the methyl group is substituted on the N-1 position. The NOESY NMR spectrum obtained for the isomer **26b** is presented in Figure 8C. Thus, we know the methylation reaction mainly happens in the N-3 position of the azabenzimidazole ring when using methyl iodide in acetone in the presence of potassium carbonate.

Chemistry. Procedures for the preparation of all final products are presented below along with representative procedures for all methods used in the preparation of intermediates. All solvents and reagents were used without purification as acquired from commercial sources. Melting points were measured using a capillary melting point apparatus which was uncorrected. The progress of the chemical reaction was monitored by thin-layer chromatography on silica gel 60-F₂₅₄ aluminum plates and detected under UV light. All NMR spectra were recorded employing a 400 MHz spectrometer, and chemical shifts (δ) are in ppm relative to TMS as internal standard. Phase-sensitive 2D NOE experiments were collected with 2048 \times 128 data points in the two dimensions and 8 scans per t_1 increment. A mixing time of 800 ms and recycle delay of 2 s were used. Spectral width was 3.4 kHz. Electrospray ionization (ESI) Q-ToF and Orbitrap were used for the high-resolution mass spectra

measurements. Elemental analyses are within ± 0.4 of the theoretical values. The compounds reported as salts frequently analyzed for fractional moles of water and/or ethanol and/or ether of solvation. In each case proton NMR showed the presence of indicated solvent(s).

4-[[[6-Amino-5-nitropyridin-2-yl)oxylmethyl]benzonitrile (2). To a solution of 4-hydroxymethylbenzonitrile (5.00 g, 37.5 mmol) and 2-amino-6-chloro-3-nitropyridine (1) (7.10 g, 41.0 mmol) in dimethylformamide (30 mL) was slowly added to sodium hydride (3.00 g, 75.0 mmol, as a 60 wt % dispersion in mineral oil). The resulting mixture was stirred at room temperature for 3 h and then poured into ice-water. The resulting precipitate was collected, washed with water, and dried to provide a yellow solid 2 (9.3 g, 92%). Mp: 182–185 °C. ^1H NMR (400 MHz, DMSO- d_6): δ 8.29 (d, 1 H, $J = 8.8$ Hz), 8.18 (br s, 2 H), 7.86 (d, 2 H, $J = 8.0$ Hz), 7.67 (d, 2 H, $J = 8.0$ Hz), 6.23 (d, 1 H, $J = 8.8$ Hz), 5.48 (s, 2 H). ^{13}C NMR (DMSO- d_6 , 75 MHz) δ_{C} 165.4, 154.1, 141.9, 138.2, 132.4, 128.9, 121.3, 118.7, 110.7, 101.0, 66.8. HR-ESI-MS: calcd for $\text{C}_{13}\text{H}_{11}\text{N}_4\text{O}_3$, m/z 271.0831 ($\text{M} + \text{H}$) $^+$, found m/z 271.0842.

4-[[[5,6-Diaminopyridin-2-yl)oxylmethyl]benzonitrile (3). A mixture of iron dust (3.72 g, 66.6 mmol), ammonium chloride (5.34 g, 99.9 mmol), and 2 (6.00 g, 22.2 mmol) in 96 mL of 2-propanol-water (5:3, v/v) was heated at reflux for 4 h. The reaction mixture was filtered, and the dark filtrate was freed from solvent by distillation under reduced pressure. The resulting residue was diluted with water and extracted with ethyl acetate (100 mL \times 3). The combined organic phases were washed with brine, dried over anhydrous sodium sulfate, filtered, and concentrated under reduced pressure. The dark solid was crystallized with methanol to give 3 (3.6 g, 68%). Mp: 146–149 °C. ^1H NMR (400 MHz, DMSO- d_6): δ 7.81 (d, 2 H, $J = 6.8$ Hz), 7.58 (s, 2 H), 6.75 (d, 1 H, $J = 6.8$ Hz), 5.87 (d, 1 H, $J = 6.8$ Hz), 5.36 (s, 2 H), 5.24 (s, 2 H), 4.15 (s, 2 H). ^{13}C NMR (DMSO- d_6 , 75 MHz) δ_{C} 153.7, 146.4, 144.4, 132.2, 128.0, 124.0, 123.2, 118.9, 109.9, 96.0, 65.3. HR-ESI-MS: calcd for $\text{C}_{13}\text{H}_{13}\text{N}_4\text{O}$, m/z 241.1089 ($\text{M} + \text{H}$) $^+$, found m/z 241.1082.

Ethyl 2-(4-Cyanophenoxy)acetate (5). To a stirred solution of 4-cyanophenol 4 (11.9 g, 0.10 mol) in acetone were added potassium carbonate (24.9 g, 0.18 mol) and ethyl bromoacetate (13.7 mL, 0.14 mol) at room temperature. The mixture was stirred at room temperature for 12 h. The mixture was filtered, the filtrate was evaporated, and the resulting residue was dissolved in water (50 mL). The aqueous layer was extracted with ethyl acetate (100 mL \times 3). The combined organic phases were washed with brine, dried over anhydrous sodium sulfate, filtered, and concentrated under reduced pressure. Crystallization from the hexanes/ethyl acetate (10:1, v/v) mixture gave a white solid 5 (16.0 g, 78%). Mp: 54–55 °C. ^1H NMR (400 MHz, CDCl_3): δ 7.61 (d, 2 H, $J = 8.4$ Hz), 6.96 (d, 2 H, $J = 8.4$ Hz), 4.68 (s, 2 H), 4.28 (q, 2 H, $J = 7.6$ Hz), 1.30 (t, 3 H, $J = 7.6$ Hz).

(4-Cyanophenoxy)acetic Acid (6). A solution of 2 M sodium hydroxide (10 mL, 20 mmol) was added dropwise to a solution of ethyl 2-(4-cyanophenoxy)acetate 5 (2.05 g, 10 mmol) in methanol (40 mL) at room temperature. After 1 h, the solution was concentrated and the obtained residue was dissolved in water and then acidified with 1 N HCl. The precipitate was collected and washed with water and afforded a white solid 6 (1.42 g, 80%). Mp: 178–179 °C (lit.³⁰ 175–178 °C). ^1H NMR (400 MHz, DMSO- d_6): δ 13.15 (s, 1H), 7.76 (s, 2 H), 7.09 (s, 2 H), 4.81 (s, 2H).

N-[2-Amino-6-[(4-cyanobenzyl)oxy]pyridin-3-yl]-2-(4-cyanophenoxy)acetamide (7). A solution of 6 (4.09 g, 23.1 mmol), thionyl chloride (3.4 mL, 46.2 mmol), and DMF (0.1 mL) in toluene (50 mL) was heated at reflux for 6 h. The solution was concentrated to dryness under reduced pressure. Then dichloromethane (15 mL \times 2) was added, and the solvent was distilled in vacuum to yield 4.27 g of the acid chloride, which was used in the next step without further purification. The acid chloride was slowly added to the solution of 3 (4.80 g, 20.0 mmol) and triethylamine (3.3 mL, 23.7 mmol) in dichloromethane (100 mL), and the mixture was stirred at room temperature overnight. The resulting precipitate was collected, washed with dichloromethane and water, and dried to provide a light yellow solid 7 (5.83 g, 73%). Mp: 227–229 °C. ^1H NMR (400 MHz, DMSO- d_6): δ 9.26 (s, 1 H), 7.84–7.79 (m, 4 H), 7.60 (d, 2 H, $J = 7.4$ Hz), 7.30 (d, 1 H, $J = 7.6$ Hz), 7.17 (d, 2 H, $J = 7.4$ Hz), 6.03 (d, 1 H, $J = 7.6$ Hz), 5.85 (s, 2 H), 5.35 (s, 2 H), 4.79 (s, 2 H). ^{13}C NMR (DMSO- d_6 , 75

MHz): δ_{C} 166.4, 161.4, 159.7, 153.2, 143.6, 137.9, 134.1, 132.2, 128.2, 119.0, 118.8, 115.8, 110.2, 109.7, 103.3, 96.3, 66.9, 65.4; HR-ESI-MS: calcd for $\text{C}_{22}\text{H}_{18}\text{N}_5\text{O}_3$, m/z 400.1410 ($\text{M} + \text{H}$) $^+$, found m/z 400.1412.

4-[[[5-(4-Cyanobenzoyloxy)-3H-imidazo[4,5-b]pyridin-2-yl]-methoxy]benzonitrile (8). A solution of 7 (0.32 g, 0.80 mmol) in glacial acetic acid (15 mL) was heated at reflux for 12 h. The solution was concentrated to dryness under reduced pressure. The residue was vigorously stirred in 1 M ammonia solution (30 mL) for 1 h. The resulting precipitate was collected, washed with water, and purified by column chromatography (silica gel, using a gradient elution method with a mixture of dichloromethane and methanol) to afford the title compound as a light yellow solid 8 (0.26 g, 85%). Mp: 212–213 °C. ^1H NMR (400 MHz, DMSO- $d_6 + \text{D}_2\text{O}$): δ 7.91 (d, 1 H, $J = 8.4$ Hz), 7.82 (d, 2 H, $J = 8.0$ Hz), 7.77 (d, 2 H, $J = 8.4$ Hz), 7.63 (d, 2 H, $J = 8.0$ Hz), 7.23 (d, 2 H, $J = 8.4$ Hz), 6.77 (d, 1 H, $J = 8.4$ Hz), 5.47 (s, 2 H), 5.35 (s, 2 H). ^{13}C NMR (DMSO- d_6 , 75 MHz) δ_{C} 161.4, 159.5, 149.4, 143.6, 134.4, 132.4, 128.2, 119.1, 118.9, 116.1, 110.3, 106.0, 103.6, 66.1, 64.3. HR-ESI-MS: calcd for $\text{C}_{22}\text{H}_{16}\text{N}_5\text{O}_2$, m/z 382.1304 ($\text{M} + \text{H}$) $^+$, found m/z 382.1305.

General Procedure for the Pinner Method of Synthesis of Diamidine Hydrochlorides (9, 12a–c, 17a–c, 21, 25a, and 27a).

The dinitrile compounds (0.85 mmol) were suspended in saturated ethanolic HCl (30 mL) and stirred at room temperature for 3 days, isolated from air and moisture. Dry ether was added, and the solid was filtered, dried under vacuum for 5 h, and dissolved in absolute ethanol (25 mL), ammonia gas was passed for 15 min while cooling in an ice bath, and the resulting solution was stirred for 3 days at room temperature. Dry ether was added, and the precipitated solid was filtered. The crude diamidine salt was purified by neutralization with 1 M sodium hydroxide followed by filtration of the resultant solid, washed with water, and dried. Finally, the free base was stirred with anhydrous ethanolic HCl for 3 days and diluted with ether, and the solid formed was filtered and dried and crystallized from a methanol/acetone mixture to give the diamidine HCl salt.

Trihydrochloride Salt of 4-[[[5-(4-carbamimidoylbenzyloxy)-3H-imidazo[4,5-b]pyridine-2-yl]methoxy]benzimidamide (9). White solid (0.35 g, 71%). Mp >270 °C. ^1H NMR (400 MHz, DMSO- d_6): δ 9.37 (s, 2 H), 9.23 (s, 2 H), 9.10 (s, 2 H), 8.95 (s, 2 H), 7.99 (d, 1 H, $J = 8.8$ Hz), 7.86–7.82 (m, 4 H), 7.68 (d, 2 H, $J = 8.0$ Hz), 7.30 (d, 2 H, $J = 8.8$ Hz), 6.85 (d, 1 H, $J = 8.8$ Hz), 5.51 (s, 2 H), 5.45 (s, 2 H). ^{13}C NMR (DMSO- d_6 , 75 MHz) δ_{C} 165.6, 164.9, 162.0, 160.9, 148.8, 146.2, 143.8, 130.6, 128.6, 128.2, 127.4, 123.3, 120.9, 120.8, 115.6, 108.6, 66.9, 63.0. HR-ESI-MS: calcd for $\text{C}_{22}\text{H}_{23}\text{N}_7\text{O}_2$, m/z 416.1835 ($\text{M} + \text{H}$) $^+$, found m/z 416.1844. Anal. Calcd for $\text{C}_{22}\text{H}_{23}\text{N}_7\text{O}_2 \cdot 3\text{HCl} \cdot 2.80\text{H}_2\text{O}$: C, 45.93; H, 5.19; N, 17.04. Found: C, 46.26; H, 5.01; N, 16.68.

4-[5-[(4-Cyanobenzyl)oxy]-3H-imidazo[4,5-b]pyridin-2-yl]-benzonitrile (11a). Sodium bisulfite (0.16 g, 1.5 mmol) was added to a stirred mixture of 3 (0.24 g, 1.0 mmol) and 4-cyanobenzaldehyde (0.13 g, 1.0 mmol) in dry dimethylformamide. The vigorously stirred mixture was heated at 140 °C for 12 h under a nitrogen atmosphere. The residue was poured into water and the precipitated solid was filtered and crystallized from methanol to give the title compound 11a as a yellow solid (0.26 g, 75%). Mp: >285 °C. ^1H NMR (400 MHz, DMSO- d_6): δ 13.73 (s, 0.7 H), 13.40 (s, 0.3 H), 8.30 (d, 2 H, $J = 8.4$ Hz), 8.01–8.12 (m, 3 H), 7.86 (d, 2 H, $J = 8.0$ Hz), 7.66 (d, 2 H, $J = 8.0$ Hz), 6.87 (d, 1 H, $J = 8.4$ Hz), 5.53 (s, 2 H). ^{13}C NMR (DMSO- d_6 , 75 MHz) δ_{C} 160.3, 150.0, 143.9, 135.0, 133.3, 132.8, 128.5, 127.2, 119.3, 119.2, 112.0, 110.6, 107.1, 66.6. HR-ESI-MS: calcd for $\text{C}_{21}\text{H}_{14}\text{N}_5\text{O}$, m/z 352.1198 ($\text{M} + \text{H}$) $^+$, found m/z 352.1203.

3-[5-[(4-Cyanobenzyl)oxy]-3H-imidazo[4,5-b]pyridin-2-yl]-benzonitrile (11b). This compound was prepared using the same procedure as for the preparation of 11a. Yellow solid (yield, 83%). Mp: 246–247 °C. ^1H NMR (400 MHz, DMSO- d_6): δ 13.64 (s, 0.6 H), 13.32 (s, 0.4 H), 8.52 (s, 1 H), 8.45 (d, 1 H, $J = 8.4$ Hz), 7.96–8.09 (m, 2 H), 7.86 (d, 2 H, $J = 8.0$ Hz), 7.75–7.77 (m, 1 H), 7.66 (d, 2 H, $J = 8.0$ Hz), 6.86 (d, 1 H, $J = 8.4$ Hz), 5.53 (s, 2 H). ^{13}C NMR (DMSO- d_6 , 75 MHz) δ_{C} 160.4, 154.5, 143.8, 133.7, 132.8, 131.3, 131.1, 130.9, 129.9, 128.6, 119.3, 118.9, 112.6, 110.6, 107.4, 66.6. HR-ESI-MS: calcd for $\text{C}_{21}\text{H}_{14}\text{N}_5\text{O}$, m/z 352.1198 ($\text{M} + \text{H}$) $^+$, found m/z 352.1188.

Ethyl 3-[5-[(4-Cyanobenzyl)oxy]-3H-imidazo[4,5-b]pyridin-2-yl]-benzoate (11c). This compound was prepared using the same procedure as for the preparation of 11a. Yellow solid (yield, 85%). Mp: 234–235 °C. ¹H NMR (400 MHz, DMSO-*d*₆): δ 8.28 (d, 2 H, *J* = 8.4 Hz), 8.08 (d, 2 H, *J* = 8.4 Hz), 8.02 (d, 1 H, *J* = 8.4 Hz), 7.86 (d, 2 H, *J* = 8.0 Hz), 7.66 (d, 2 H, *J* = 8.0 Hz), 6.86 (d, 1 H, *J* = 8.4 Hz), 5.52 (s, 2 H), 3.88 (s, 3 H). ¹³C NMR (DMSO-*d*₆, 75 MHz) δ_C 165.8, 160.0, 149.3, 143.3, 133.9, 132.4, 130.4, 129.8, 128.1, 126.4, 118.8, 110.3, 106.8, 66.2, 52.3. HR-ESI-MS: calcd for C₂₂H₁₇N₄O₃, *m/z* 385.1301 (M + H)⁺, found *m/z* 385.1292.

Dihydrochloride Salt of 4-[5-[(4-Carbamimidoylbenzyl)oxy]-3H-imidazo[4,5-b]pyridin-2-yl]benzimidamide (12a). This compound was prepared using the same procedure as for the preparation of 9. Yellow solid (0.28 g, 67%). Mp: >290 °C. ¹H NMR (400 MHz, DMSO-*d*₆ + D₂O): δ 8.30 (d, 2 H, *J* = 8.0 Hz), 7.96 (d, 1 H, *J* = 8.8 Hz), 7.89 (d, 2 H, *J* = 8.4 Hz), 7.78 (d, 2 H, *J* = 8.0 Hz), 7.66 (d, 2 H, *J* = 8.4 Hz), 6.78 (d, 1 H, *J* = 8.8 Hz), 5.52 (s, 2 H). ¹³C NMR (DMSO-*d*₆ + D₂O, 75 MHz) δ_C 165.7, 165.4, 160.5, 149.7, 144.3, 134.9, 129.3, 129.1, 128.6, 128.2, 127.5, 126.9, 107.5, 66.6; HR-ESI-MS: calcd for C₂₁H₂₀N₇O *m/z* 386.1729 (M + H)⁺, found *m/z* 386.1736. Anal. Calcd for C₂₁H₁₉N₇O · 2HCl · 1.97H₂O: C, 51.08; H, 5.09; N, 19.85. Found: C, 51.46; H, 4.94; N, 19.47.

Trihydrochloride Salt of 3-[5-[(4-Carbamimidoylbenzyl)oxy]-3H-imidazo[4,5-b]pyridin-2-yl]benzimidamide (12b). This compound was prepared using the same procedure as for the preparation of 9. Light-green solid (0.26 g, 61%). Mp: >260 °C. ¹H NMR (400 MHz, DMSO-*d*₆): δ 13.70 (s, 0.6 H), 13.52 (s, 0.4 H), 9.50 (d, 2 H, *J* = 9.2 Hz), 9.34 (d, 2 H, *J* = 7.2 Hz), 9.17 (d, 2 H, *J* = 9.2 Hz), 9.02 (d, 2 H, *J* = 10.4 Hz), 8.62 (s, 1 H, *J* = 8.0 Hz), 8.44 (d, 1 H, *J* = 8.4 Hz), 8.08, 7.98 (dd, 1 H, *J* = 8.4 Hz), 7.78–7.89 (m, 4 H), 7.70 (d, 2 H, *J* = 8.0 Hz), 6.87 (d, 1 H, *J* = 8.4 Hz), 5.55 (s, 2 H). ¹³C NMR (DMSO-*d*₆ + D₂O, 75 MHz) δ_C 165.5, 165.4, 160.1, 149.7, 144.0, 131.0, 130.8, 130.1, 129.4, 129.4, 128.4, 127.9, 127.3, 126.2, 106.9, 66.4. HR-ESI-MS: calcd for C₂₁H₂₀N₇O *m/z* 386.1729 (M + H)⁺, found *m/z* 386.1723. Anal. Calcd for C₂₁H₁₉N₇O · 3HCl · 0.5EtOH: C, 51.02; H, 4.87; N, 18.93. Found: C, 50.81; H, 4.98; N, 18.83.

Hydrochloride Salt of Ethyl 4-[5-[(4-Carbamimidoylbenzyl)oxy]-3H-imidazo[4,5-b]pyridin-2-yl]benzoate (12c). This compound was prepared using the same procedure as for the preparation of 9. Yellow solid (0.31 g, 75%). Mp: >235 °C. ¹H NMR (400 MHz, DMSO-*d*₆ + D₂O): δ 8.25 (d, 2 H, *J* = 8.4 Hz), 8.08 (d, 2 H, *J* = 8.4 Hz), 8.00 (d, 1 H, *J* = 8.4 Hz), 7.79 (d, 2 H, *J* = 8.0 Hz), 7.68 (d, 2 H, *J* = 8.0 Hz), 6.85 (d, 1 H, *J* = 8.4 Hz), 5.54 (s, 2 H), 4.33 (q, 2 H, *J* = 7.2 Hz), 1.33 (t, 3 H, *J* = 7.2 Hz). ¹³C NMR (DMSO-*d*₆ + D₂O, 75 MHz) δ_C 165.4, 165.2, 160.3, 149.1, 143.6, 133.0, 131.0, 129.8, 128.3, 127.7, 127.3, 126.6, 107.4, 66.4, 61.0, 14.0. HR-ESI-MS: calcd for C₂₃H₂₂N₃O₃ *m/z* 416.1723 (M + H)⁺, found *m/z* 416.1728. Anal. Calcd for C₂₃H₂₁N₃O₃ · HCl · 1.9H₂O: C, 56.83; H, 5.35; N, 14.41. Found: C, 56.53; H, 5.11; N, 14.25.

6-Chloro-2,3-diaminopyridine (13). A mixture of 2-amino-6-chloro-3-nitropyridine (1) (6.0 g, 34.6 mmol), tin(II) chloride dihydrate (39.0 g, 0.17 mol), and 180 mL of ethyl acetate and 2-propanol (9:1, v/v) was stirred at 60 °C for 1 h, after which sodium borohydride (0.66 g, 17.5 mmol) was added at 60 °C, and the mixture was stirred for another 3 h at the same temperature. The solution was concentrated to dryness under reduced pressure. The resulting residue was diluted with water, neutralized by adding aqueous solution of potassium carbonate, and extracted with ethyl acetate (50 mL × 3). The combined organic phases were washed with brine, dried over anhydrous sodium sulfate, filtered, concentrated, and crystallized from ethyl acetate and hexane to give the title compound 13 as a white solid (3.3 g, 70%). Mp: 119–120 °C (lit.³⁷ mp 120–122 °C). ¹H NMR (400 MHz, DMSO-*d*₆): δ 6.68 (d, 2 H, *J* = 7.6 Hz), 6.34 (d, 1 H, *J* = 7.6 Hz), 5.78 (s, 2 H), 4.76 (s, 2 H). HR-ESI-MS: calcd for C₅H₇N₃Cl *m/z* 144.0329 (M + H)⁺, found *m/z* 144.0335.

N-(2-Amino-6-chloropyridin-3-yl)-2-[(4-cyanophenoxy)acetamide (14a). A solution of (4-cyanophenoxy)acetic acid (1.01 g, 6.27 mmol) and CDI (1.02 g, 6.27 mmol) in 50 mL of tetrahydrofuran (THF) was stirred at 50 °C for 30 min. The 6-chloro-2,3-diaminopyridine (13) (0.87 g, 6.08 mmol) in 400 mL of THF was added, and the resulting solution was stirred for another 6 h at 50 °C. The solution was concentrated to dryness under reduced pressure. Ethyl acetate (50 mL)

and water (50 mL) were subsequently added, and the precipitate was collected to afford the title compound 14a as a white solid (1.28 g, 70%). Mp: 215–217 °C. ¹H NMR (400 MHz, DMSO-*d*₆): δ 9.43 (s, 1 H), 7.79 (d, 2 H, *J* = 8.8 Hz), 7.48 (d, 1 H, *J* = 8.0 Hz), 7.17 (d, 2 H, *J* = 8.8 Hz), 6.57 (d, 1 H, *J* = 8.0 Hz), 6.34 (s, 2 H), 4.83 (s, 2 H). ¹³C NMR (DMSO-*d*₆, 75 MHz) δ_C 166.5, 161.3, 154.3, 144.4, 135.6, 134.1, 119.0, 116.2, 115.8, 110.4, 103.3, 66.8. HR-ESI-MS: calcd for C₁₄H₁₂ClN₄O₂ *m/z* 303.0649 (M + H)⁺, found *m/z* 303.0647.

N-(2-Amino-6-chloropyridin-3-yl)-3-(4-cyanophenyl)propanamide (14b). This compound was prepared using the same procedure as for the preparation of 14a. White solid (yield, 83%). Mp: 229–230 °C. ¹H NMR (400 MHz, DMSO-*d*₆): δ 9.11 (s, 1 H), 7.76 (d, 2 H, *J* = 8.0 Hz), 7.56 (d, 1 H, *J* = 8.0 Hz), 7.46 (d, 2 H, *J* = 8.0 Hz), 6.55 (d, 1 H, *J* = 8.0 Hz), 6.21 (s, 2 H), 2.98 (t, 2 H, *J* = 7.4 Hz), 2.67 (t, 2 H, *J* = 7.4 Hz). ¹³C NMR (DMSO-*d*₆, 75 MHz) δ_C 170.6, 153.5, 147.3, 143.6, 134.5, 132.2, 129.4, 119.0, 117.2, 110.5, 108.9, 36.5, 30.7. HR-ESI-MS: calcd for C₁₅H₁₄ClN₄O *m/z* 301.0856 (M + H)⁺, found *m/z* 301.0858.

N-(2-Amino-6-chloropyridin-3-yl)-2-[(4-cyanophenyl)amino]acetamide (14c). This compound was prepared using the same procedure as for the preparation of 14a. White solid (yield, 65%). Mp: 257–258 °C. ¹H NMR (400 MHz, DMSO-*d*₆): δ 9.30 (s, 1 H), 7.53–7.47 (m, 3 H), 6.97 (s, 1 H), 6.69 (d, 2 H, *J* = 7.2 Hz), 6.56 (d, 1 H, *J* = 7.2 Hz), 6.30 (s, 2 H), 4.00 (s, 2 H). ¹³C NMR (DMSO-*d*₆, 75 MHz) δ_C 168.8, 154.1, 152.0, 144.1, 135.2, 133.3, 120.5, 116.7, 112.2, 110.5, 96.4, 45.7. HR-ESI-MS: calcd for C₁₄H₁₃ClN₅O *m/z* 302.0809 (M + H)⁺, found *m/z* 302.0799.

N-[2-Amino-6-(4-cyanophenyl)pyridin-3-yl]-2-(4-cyanophenoxy)acetamide (15a). To a suspension of 4-cyanophenyl boronic acid (0.35 g, 2.4 mmol), an aqueous solution of Na₂CO₃ (2.3 mL, 2 M, deaired), ethanol (3 mL), 14a (0.45 g, 1.5 mmol) in deaired dioxane (30 mL), and tetrakis(triphenylphosphine) palladium [Pd(PPh₃)₄, 0.14 g, 0.12 mmol] was added under an atmosphere of nitrogen. The vigorously stirred mixture was warmed to 80 °C for 24 h. The solvent was evaporated under reduced pressure, and the resulting residue was diluted with ethyl acetate (50 mL) and 2 M aqueous Na₂CO₃ (15 mL) containing 5 mL of concentrated ammonia. The precipitate was collected to afford the title compound 15a as a yellow solid (0.42 g, 77%). Mp: 222–224 °C. ¹H NMR (400 MHz, DMSO-*d*₆): δ 9.52 (s, 1 H), 8.17 (d, 2 H, *J* = 8.4 Hz), 7.89 (d, 2 H, *J* = 8.4 Hz), 7.81 (d, 2 H, *J* = 8.8 Hz), 7.70 (d, 1 H, *J* = 8.0 Hz), 7.29 (d, 1 H, *J* = 8.0 Hz), 7.19 (d, 2 H, *J* = 8.8 Hz), 6.13 (s, 2 H), 4.89 (s, 2 H). ¹³C NMR (DMSO-*d*₆, 75 MHz) δ_C 166.5, 161.4, 153.5, 148.9, 143.0, 134.1, 133.1, 132.5, 126.8, 119.0, 118.9, 118.0, 115.8, 110.5, 109.7, 103.4, 66.9. HR-ESI-MS: calcd for C₂₁H₁₆N₃O₂ *m/z* 370.1304 (M + H)⁺, found *m/z* 370.1299.

N-[2-Amino-6-(4-cyanophenyl)pyridin-3-yl]-3-(4-cyanophenyl)propanamide (15b). This compound was prepared using a procedure similar to that for the preparation of 15a except the catalyst [1,1'-bis(diphenylphosphino)ferrocene]dichloropalladium(II) [Pd(dppf)Cl₂] instead of Pd(PPh₃)₄ was used. Gray solid (yield, 67%). Mp: 241–242 °C. ¹H NMR (400 MHz, DMSO-*d*₆): δ 9.33 (s, 1 H), 8.15 (d, 2 H, *J* = 8.0 Hz), 7.76–7.89 (m, 5 H), 7.48 (d, 2 H, *J* = 7.6 Hz), 7.27 (d, 1 H, *J* = 7.6 Hz), 6.06 (s, 2 H), 2.74–2.76 (m, 2 H), 2.63–2.69 (m, 2 H). ¹³C NMR (DMSO-*d*₆, 75 MHz) δ_C 170.7, 152.2, 147.5, 147.4, 143.1, 132.4, 132.2, 131.1, 129.5, 126.6, 119.3, 119.0, 110.3, 109.7, 108.8, 36.7, 30.9. HR-ESI-MS: calcd for C₂₂H₁₈N₃O *m/z* 368.1511 (M + H)⁺, found *m/z* 368.1503.

N-[2-Amino-6-(4-cyanophenyl)pyridin-3-yl]-2-[(4-cyanophenyl)amino]acetamide (15c). This compound was prepared using the same procedure as for the preparation of 15a using the catalyst Pd(dppf)Cl₂ instead of Pd(PPh₃)₄. Yellow solid (yield, 62%). Mp: 243–245 °C. ¹H NMR (400 MHz, DMSO-*d*₆): δ 9.41 (s, 1 H), 8.16 (s, 2 H), 7.89 (s, 2 H), 7.77 (s, 1 H), 7.50 (s, 2 H), 7.28 (s, 1 H), 7.02 (s, 1 H), 6.71 (s, 2 H), 6.10 (s, 2 H), 4.05 (s, 2 H). ¹³C NMR (DMSO-*d*₆, 75 MHz) δ_C 168.8, 152.9, 152.0, 148.3, 143.0, 133.4, 132.5, 132.1, 126.7, 120.5, 119.0, 118.7, 112.2, 110.4, 109.8, 96.4, 45.9. HR-ESI-MS: calcd for C₂₁H₁₇N₆O *m/z* 369.1464 (M + H)⁺, found *m/z* 369.1458.

4-[2-[(4-Cyanophenoxy)methyl]-3H-imidazo[4,5-b]pyridin-5-yl]-benzotrile (16a). The dinitrile intermediate 15a (0.31 g, 0.84 mmol) was dissolved in glacial acetic acid (15 mL) heated at reflux for 6 h. The solution was then concentrated to dryness, and the residue was

vigorously stirred in ammonia solution (1 M, 30 mL). The resulting precipitate was collected, washed with water, and purified by column chromatography (silica gel, using a gradient elution method with a mixture of dichloromethane and methanol) to afford the title compound as a light yellow solid **16a** (0.23 g, 78%). Mp: 260–262 °C. ¹H NMR (400 MHz, DMSO-*d*₆+D₂O): δ 8.27 (d, 2 H, *J* = 8.0 Hz), 8.04 (d, 1 H, *J* = 8.4 Hz), 7.90 (t, 3 H, *J* = 8.0 Hz, 8.4 Hz), 7.77 (d, 2 H, *J* = 8.4 Hz), 7.25 (d, 2 H, *J* = 8.4 Hz), 5.45 (s, 2 H). ¹³C NMR (DMSO-*d*₆, 75 MHz) δ_C 161.8, 155.5, 148.1, 144.4, 134.5, 133.0, 127.5, 124.6, 119.4, 116.3, 115.5, 110.6, 103.6, 65.1. HR-ESI-MS: calcd for C₂₁H₁₄N₅O *m/z* 352.1198 (M + H)⁺, found *m/z* 352.1206.

4-[2-(4-Cyanophenethyl)-3H-imidazo[4,5-*b*]pyridin-5-yl]benzonitrile (16b). This compound was prepared using the same procedure as for the preparation of **16a**. Brown solid, (yield, 85%). Mp: 235–237 °C. ¹H NMR (400 MHz, DMSO-*d*₆): δ 13.07 (s, 0.6 H), 12.67 (s, 0.4 H), 8.7 (d, 2 H, *J* = 8.0 Hz), 7.89–8.05 (m, 4 H), 7.74 (d, 2 H, *J* = 8.0 Hz), 7.47 (d, 2 H, *J* = 8.0 Hz), 3.24 (s, 4 H). ¹³C NMR (DMSO-*d*₆, 75 MHz) δ_C 158.2, 148.1, 147.1, 144.1, 133.0, 132.6, 129.8, 127.5, 119.3, 119.3, 115.8, 110.8, 109.3, 33.1, 30.2. HR-ESI-MS: calcd for C₂₂H₁₆N₅ *m/z* 350.1406 (M + H)⁺, found *m/z* 350.1412.

4-[[5-(4-Cyanophenyl)-3H-imidazo[4,5-*b*]pyridin-2-yl]methylamino]benzonitrile (16c). This compound was prepared using the same procedure as for the preparation of **16a**. Yellow solid (yield, 73%). Mp: 237–239 °C. ¹H NMR (400 MHz, DMSO-*d*₆): δ 8.28 (d, 2 H, *J* = 8.4 Hz), 8.02 (d, 1 H, *J* = 7.6 Hz), 7.91–7.95 (m, 3 H), 7.48 (d, 2 H, *J* = 8.8 Hz), 7.37 (br s, 1 H), 6.74 (d, 2 H, *J* = 8.8 Hz), 4.63 (s, 2 H). ¹³C NMR (DMSO-*d*₆, 75 MHz) δ_C 157.2, 152.1, 148.8, 144.2, 133.9, 133.2, 127.8, 121.0, 119.5, 116.3, 112.9, 111.0, 97.3, 41.4. HR-ESI-MS: calcd for C₂₁H₁₅N₆ *m/z* 351.1358 (M + H)⁺, found *m/z* 351.1351.

Trihydrochloride Salt of 4-[2-[(4-Carbamimidoylphenoxy)methyl]-3H-imidazo[4,5-*b*]pyridin-5-yl]benzimidamide (17a). This compound was prepared using the same procedure as for the preparation of **9**. Yellow solid (0.29 g, 66%). Mp: >290 °C. ¹H NMR (400 MHz, DMSO-*d*₆): δ 13.69 (s, 0.6 H), 13.43 (s, 0.4 H), 9.52 (s, 2 H), 9.31 (s, 4 H), 9.13 (s, 2 H), 8.34 (d, 2 H, *J* = 7.2 Hz), 8.17–7.88 (m, 6 H), 7.33 (d, 2 H, *J* = 7.6 Hz), 5.55 (s, 2 H). ¹³C NMR (DMSO-*d*₆, 75 MHz) δ_C 165.3, 164.7, 162.3, 153.2, 149.3, 144.4, 130.4, 128.9, 127.6, 127.1, 120.5, 116.3, 115.5, 64.2. HR-ESI-MS: calcd for C₂₁H₂₀N₇O *m/z* 386.1729 (M + H)⁺, found *m/z* 386.1741. Anal. Calcd for C₂₁H₁₉N₇O·3HCl·1.2H₂O·0.07acetone: C, 48.94; H, 4.81; N, 18.84. Found: C, 48.97; H, 4.95; N, 18.47.

Dihydrochloride Salt of 4-[2-(4-Carbamimidoylphenethyl)-3H-imidazo[4,5-*b*]pyridin-5-yl]benzimidamide (17b). This compound was prepared using the same procedure as for the preparation of **9**. White solid (0.33 g, 82%). Mp: >300 °C. ¹H NMR (400 MHz, DMSO-*d*₆): δ 9.06–9.45 (br s, 8 H), 8.32 (s, 2 H, *J* = 7.2 Hz), 7.92–8.02 (m, 4 H), 7.75 (d, 2 H, *J* = 8.4 Hz), 7.54 (s, 2 H, *J* = 7.2 Hz), 3.29 (s, 4 H). ¹³C NMR (DMSO-*d*₆, 75 MHz) δ_C 165.5, 165.4, 158.0, 148.4, 147.6, 144.7, 129.3, 129.0, 128.4, 127.4, 127.0, 125.9, 115.8, 32.8, 30.1. HR-ESI-MS: calcd for C₂₂H₂₂N₇ *m/z* 384.1937 (M + H)⁺, found *m/z* 384.1951. Anal. Calcd for C₂₂H₂₁N₇·2HCl·1.3H₂O: C, 55.07; H, 5.38; N, 20.44. Found: C, 55.29; H, 5.42; N, 20.16.

Dihydrochloride Salt of 4-[[5-(4-carbamimidoylphenyl)-3H-imidazo[4,5-*b*]pyridin-2-yl]methylamino]benzimidamide (17c). This compound was prepared using the same procedure as for the preparation of **9**. Yellow solid (0.29 g, 70%). Mp: >280 °C. ¹H NMR (400 MHz, DMSO-*d*₆): δ 13.36 (s, 0.6 H), 12.96 (s, 0.4 H), 9.44 (s, 2 H), 9.17 (s, 2 H), 8.87 (s, 2 H), 8.58 (s, 2 H), 8.33 (t, 2 H, *J* = 8.8 Hz), 8.09 (d, 0.6 H, *J* = 8.4 Hz), 7.95–7.97 (m, 3.4 H), 7.65 (d, 2 H, *J* = 6.8 Hz), 7.48–7.55 (m, 1 H, NH), 6.80 (d, 2 H, *J* = 8.8 Hz), 4.63 (dd, 2 H, *J* = 5.6 Hz). ¹³C NMR (DMSO-*d*₆, 75 MHz) δ_C 165.8, 164.8, 157.0, 153.5, 149.2, 144.8, 130.2, 129.2, 127.9, 127.5, 116.4, 114.0, 112.5, 41.4. HR-ESI-MS: calcd for C₂₁H₂₁N₈ *m/z* 385.1889 (M + H)⁺, found *m/z* 385.1894. Anal. Calcd for C₂₁H₂₀N₈·2HCl·1.7H₂O·0.04Et₂O: C, 51.77; H, 5.30; N, 22.82. Found: C, 52.09; H, 5.27; N, 22.47.

N-(2-Amino-6-chloropyridin-3-yl)-4-cyanobenzamide (18). A solution of 4-cyanobenzoic acid (1.47 g, 0.01 mol), thionyl chloride (1.4 mL, 0.02 mol), and DMF (0.1 mL) in toluene (50 mL) was heated at reflux for 2 h. The solution was concentrated to dryness under reduced pressure. Dichloromethane (15 mL × 2) was added to the solid, and the

solvent was distilled off in vacuo to yield 1.40 g of the acid chloride, which was used in the next step without further purification. The acid chloride was slowly added to the solution of **13** (1.0 g, 7.0 mmol) and triethylamine (1.5 mL, 10.0 mmol) in dichloromethane (100 mL) at room temperature and stirred overnight. The resulting precipitate was collected, washed with dichloromethane and water, and dried to provide a light yellow solid **18** (1.47 g, 77%). Mp: 258–260 °C. ¹H NMR (400 MHz, DMSO-*d*₆): δ 9.85 (s, 1 H), 8.13 (d, 2 H, *J* = 8.0 Hz), 8.01 (d, 2 H, *J* = 8.0 Hz), 7.53 (d, 1 H, *J* = 8.0 Hz), 6.61 (d, 1 H, *J* = 8.0 Hz), 6.42 (s, 2 H). ¹³C NMR (DMSO-*d*₆, 75 MHz) δ_C 164.6, 155.1, 145.2, 138.3, 137.2, 132.3, 128.8, 118.4, 116.5, 113.8, 110.4. HR-ESI-MS: calcd for C₁₃H₁₀N₄OCl *m/z* 273.0542 (M + H)⁺, found *m/z* 273.0544.

N-[2-Amino-6-(4-cyanophenyl)pyridin-3-yl]-4-cyanobenzamide (19). This compound was prepared using the same procedure as for the preparation of **15a**. Yellow solid (yield, 81%). Mp: >290 °C. ¹H NMR (400 MHz, DMSO-*d*₆): δ 9.93 (s, 1 H), 8.15–8.21 (m, 4 H), 8.01 (d, 2 H, *J* = 8.0 Hz), 7.91 (d, 2 H, *J* = 8.0 Hz), 7.76 (d, 1 H, *J* = 7.2 Hz), 7.32 (d, 1 H, *J* = 7.2 Hz), 6.18 (s, 2 H). ¹³C NMR (DMSO-*d*₆, 75 MHz) δ_C 164.7, 154.2, 149.2, 143.0, 138.6, 134.3, 132.5, 132.3, 128.8, 126.8, 119.0, 118.7, 118.4, 113.8, 110.6, 109.6. HR-ESI-MS: calcd for C₂₀H₁₄N₅O *m/z* 340.1198 (M + H)⁺, found *m/z* 340.1194.

4,4'-(3H-Imidazo[4,5-*b*]pyridine-2,5-diyl)dibenzonitrile (20). This compound was prepared using the same procedure as for the preparation of **16a**. Yellow solid (yield, 89%). Mp: >290 °C. ¹H NMR (400 MHz, DMSO-*d*₆): δ 13.93 (br s, 1 H), 8.41 (d, 2 H, *J* = 8.0 Hz), 8.34 (d, 2 H, *J* = 8.0 Hz), 8.21 (br s, 1 H), 7.97–8.08 (m, 5 H). ¹³C NMR (DMSO-*d*₆, 75 MHz) δ_C 152.1, 149.5, 143.4, 133.5, 133.0, 132.8, 127.3, 127.3, 118.9, 118.5, 116.7, 112.7, 110.9. HR-ESI-MS: calcd for C₂₀H₁₂N₅ *m/z* 322.1103 (M + H)⁺, found *m/z* 322.1093.

Trihydrochloride Salt of 4,4'-(3H-Imidazo[4,5-*b*]pyridine-2,5-diyl)dibenzimidamide (21). This compound was prepared using the same procedure as for the preparation of **9**. Yellow solid (0.25 g, 61%). Mp: >300 °C. ¹H NMR (400 MHz, DMSO-*d*₆): δ 9.50 (s, 2 H), 9.44 (s, 2 H), 9.19 (s, 2 H), 9.11 (s, 2 H), 8.49 (d, 2 H, *J* = 8.0 Hz), 8.39 (d, 2 H, *J* = 8.0 Hz), 8.23 (d, 1 H, *J* = 8.4 Hz), 7.98–8.07 (m, 5 H). ¹³C NMR (DMSO-*d*₆, 75 MHz) δ_C 165.3, 165.0, 152.4, 149.7, 144.1, 133.9, 129.7, 129.1, 128.8, 127.7, 127.1, 126.9, 116.8. HR-ESI-MS: calcd for C₂₀H₁₈N₇ *m/z* 356.1624 (M + H)⁺, found *m/z* 356.1612. Anal. Calcd for C₂₀H₁₇N₇·3HCl·1.1H₂O: C, 49.57; H, 4.62; N, 20.23. Found: C, 49.89; H, 4.67; N, 19.88.

4-[[5-Chloro-3H-imidazo[4,5-*b*]pyridin-2-yl]methoxy]benzonitrile (22). This compound was prepared using the same procedure as for the preparation of **16a**. White solid (yield, 88%). Mp: 270–272 °C. ¹H NMR (400 MHz, DMSO-*d*₆): δ 8.04 (d, 1 H, *J* = 8.0 Hz), 7.81 (d, 2 H, *J* = 8.4 Hz), 7.31 (d, 1 H, *J* = 8.0 Hz), 7.26 (d, 2 H, *J* = 8.4 Hz), 5.49 (s, 2 H). ¹³C NMR (DMSO-*d*₆, 75 MHz) δ_C 161.1, 152.6, 143.9, 134.3, 119.0, 118.1, 116.0, 103.8, 64.0. HR-ESI-MS: calcd for C₁₄H₁₀N₄OCl *m/z* 285.0543 (M + H)⁺, found *m/z* 285.0539.

4-[[5-Chloro-3-methyl-3H-imidazo[4,5-*b*]pyridin-2-yl]methoxy]benzonitrile (23a). To a suspension of **22** (1.0 g, 3.5 mmol) and anhydrous potassium carbonate (1.46 g, 10.5 mmol) in acetone (25 mL) was added a solution of methyl iodide (0.33 mL, 5.25 mmol) dissolved in acetone (25 mL) at room temperature. The reaction mixture was stirred for 12 h and filtered. The filtrate was concentrated under reduced pressure. The residue was diluted with ethyl acetate (50 mL), washed with water and saturated saline, dried over anhydrous sodium sulfate, filtered, and concentrated. The crude solid was then purified by column chromatography (silica gel, using a gradient elution method with a mixture of hexane and ethyl acetate) to afford the title compound which eluted first as a white solid **23a** (0.70 g, 67%). Mp: 199–200 °C. ¹H NMR (400 MHz, DMSO-*d*₆): δ 8.14 (d, 1 H, *J* = 8.4 Hz), 7.81 (d, 2 H, *J* = 8.8 Hz), 7.36 (d, 1 H, *J* = 8.4 Hz), 7.29 (d, 2 H, *J* = 8.8 Hz), 5.59 (s, 2 H), 3.84 (s, 3 H). ¹³C NMR (DMSO-*d*₆, 75 MHz) δ_C 161.1, 151.3, 147.4, 144.5, 134.2, 132.9, 130.4, 119.0, 118.4, 116.1, 103.8, 63.0, 28.9. HR-ESI-MS: calcd for C₁₅H₁₂N₄OCl *m/z* 299.0700 (M + H)⁺, found *m/z* 299.0713.

4-[[5-Chloro-1-methyl-1H-imidazo[4,5-*b*]pyridin-2-yl]methoxy]benzonitrile (23b). This compound, **23b**, appeared in later fractions of the chromatography as a white solid (0.07 g, 7%). Mp: 242–243 °C. ¹H NMR (400 MHz, DMSO-*d*₆): δ 8.17 (d, 1 H, *J* = 8.4 Hz), 7.82 (d, 2 H, *J*

= 8.8 Hz), 7.40 (d, 1 H, $J = 8.4$ Hz), 7.30 (d, 2 H, $J = 8.8$ Hz), 5.61 (s, 2 H), 3.91 (s, 3 H). ^{13}C NMR (DMSO- d_6 , 75 MHz): δ_{C} 161.1, 153.4, 152.5, 144.2, 134.2, 127.5, 122.4, 119.0, 118.3, 116.0, 103.8, 62.6, 30.7. HR-ESI-MS: calcd for $\text{C}_{15}\text{H}_{12}\text{N}_4\text{OCl}$ m/z 299.0700 ($\text{M} + \text{H}$) $^+$, found m/z 299.0711.

4-[2-[(4-Cyanophenoxy)methyl]-3-methyl-3H-imidazo[4,5-b]pyridin-5-yl]benzotrile (24a). This compound was prepared using the same procedure as for the preparation of 15a. Yellow solid (yield, 88%). Mp: 226–228 °C. ^1H NMR (400 MHz, DMSO- d_6): δ 8.39 (d, 2 H, $J = 8.4$ Hz), 8.21 (d, 1 H, $J = 8.4$ Hz), 8.03 (d, 1 H, $J = 8.4$ Hz), 7.98 (d, 2 H, $J = 8.4$ Hz), 7.82 (d, 2 H, $J = 8.8$ Hz), 7.32 (d, 2 H, $J = 8.8$ Hz), 5.64 (s, 2 H), 3.95 (s, 3 H). ^{13}C NMR (DMSO- d_6 , 75 MHz): δ_{C} 161.2, 152.0, 148.9, 148.3, 143.0, 134.2, 134.0, 132.8, 128.2, 127.4, 119.0, 118.9, 116.2, 116.0, 111.0, 103.8, 63.2, 28.6; HR-ESI-MS: calcd for $\text{C}_{22}\text{H}_{16}\text{N}_5\text{O}$, m/z 366.1355 ($\text{M} + \text{H}$) $^+$, found m/z 366.1363.

Dihydrochloride Salt of 4-[2-[(4-Carbamimidoylphenoxy)methyl]-3-methyl-3H-imidazo[4,5-b]pyridin-5-yl]benzimidamide (25a). This compound was prepared using the same procedure as for the preparation of 9. White solid (0.34 g, 81%). Mp: >280 °C. ^1H NMR (400 MHz, DMSO- d_6): δ 9.36 (br s, 8 H), 8.41 (d, 2 H, $J = 8.4$ Hz), 8.22 (d, 1 H, $J = 8.4$ Hz), 8.06 (d, 1 H, $J = 8.4$ Hz), 8.01 (d, 2 H, $J = 8.4$ Hz), 7.90 (d, 2 H, $J = 8.4$ Hz), 7.36 (d, 2 H, $J = 8.4$ Hz), 5.68 (s, 2 H), 3.98 (s, 3 H). ^{13}C NMR (DMSO- d_6 , 75 MHz): δ_{C} 165.2, 164.7, 162.0, 152.1, 149.1, 148.3, 143.6, 134.0, 130.2, 128.7, 128.2, 127.8, 126.9, 120.5, 116.2, 115.3, 63.2, 28.7; HR-ESI-MS: calcd for $\text{C}_{22}\text{H}_{22}\text{N}_7\text{O}$ m/z 400.1886 ($\text{M} + \text{H}$) $^+$, found m/z 400.1893 Anal. Calcd for $\text{C}_{22}\text{H}_{21}\text{N}_7\text{O} \cdot 2\text{HCl} \cdot 1.3\text{H}_2\text{O}$: C, 53.30; H, 5.20; N, 19.78. Found: C, 53.59; H, 5.15; N, 19.51.

4-[5-[(4-Cyanobenzyl)oxy]-3-methyl-3H-imidazo[4,5-b]pyridin-2-yl]benzotrile (26a). This compound was prepared using the same procedure as for the preparation of 23a. The compound 26a was purified by column chromatography (silica gel, using a gradient elution method with a mixture of hexane and ethyl acetate) which eluted first as a white solid (yield, 72%). Mp: 240–241 °C. ^1H NMR (400 MHz, DMSO- d_6): δ 8.05–8.11 (m, 5 H), 7.86 (d, 2 H, $J = 7.2$ Hz), 7.71 (d, 2 H, $J = 7.2$ Hz), 6.88 (d, 1 H, $J = 8.4$ Hz), 5.58 (s, 2 H), 3.89 (s, 3 H). ^{13}C NMR (DMSO- d_6 , 75 MHz) δ_{C} 160.0, 149.7, 145.9, 143.2, 134.4, 132.7, 132.4, 130.9, 129.9, 129.5, 128.5, 118.8, 118.5, 112.0, 110.4, 106.7, 66.5, 30.5. HR-ESI-MS: calcd for $\text{C}_{22}\text{H}_{16}\text{N}_5\text{O}$, m/z 366.1355 ($\text{M} + \text{H}$) $^+$, found m/z 366.1356.

4-[5-[(4-Cyanobenzyl)oxy]-1-methyl-1H-imidazo[4,5-b]pyridin-2-yl]benzotrile (26b). This compound, 26b, appeared in later fractions of the chromatography as a white solid (yield, 4%). Mp: 222–223 °C. ^1H NMR (400 MHz, DMSO- d_6): δ 8.07–8.15 (m, 5 H), 7.85 (d, 2 H, $J = 6.4$ Hz), 7.68 (d, 2 H, $J = 6.4$ Hz), 6.94 (d, 1 H, $J = 6.8$ Hz), 5.54 (s, 2 H), 3.94 (s, 3 H). ^{13}C NMR (DMSO- d_6 , 75 MHz): δ_{C} 159.9, 151.5, 143.6, 134.1, 132.7, 132.4, 130.0, 128.1, 125.0, 123.2, 118.9, 112.2, 110.2, 106.9, 66.0, 32.3. HR-ESI-MS: calcd for $\text{C}_{22}\text{H}_{16}\text{N}_5\text{O}$ m/z 366.1355 ($\text{M} + \text{H}$) $^+$, found m/z 366.1355.

Dihydrochloride Salt of 4-[5-[(4-Carbamimidoylbenzyl)oxy]-3-methyl-3H-imidazo[4,5-b]pyridin-2-yl]benzimidamide (27a). This compound was prepared using the same procedure as for the preparation of 9. White solid (0.27 g, 65%). Mp: >260 °C. ^1H NMR (400 MHz, DMSO- d_6): δ 9.54 (s, 2 H), 9.40 (s, 2 H), 9.28 (s, 2 H), 9.16 (s, 2 H), 8.11–8.16 (m, 3 H), 8.02 (d, 2 H, $J = 8.0$ Hz), 7.85 (d, 2 H, $J = 8.0$ Hz), 7.75 (d, 2 H, $J = 8.0$ Hz), 6.90 (d, 1 H, $J = 8.4$ Hz), 5.61 (s, 2 H), 3.93 (s, 3 H). ^{13}C NMR (DMSO- d_6 , 75 MHz) δ_{C} 165.4, 165.2, 160.0, 149.8, 145.8, 143.6, 134.7, 130.8, 129.6, 129.1, 128.8, 128.6, 128.3, 128.1, 127.3, 106.8, 66.5, 30.5. HR-ESI-MS: calcd for $\text{C}_{22}\text{H}_{22}\text{N}_7\text{O}$ m/z 400.1886 ($\text{M} + \text{H}$) $^+$, found m/z 400.1881 Anal. Calcd for $\text{C}_{22}\text{H}_{21}\text{N}_7\text{O} \cdot 2\text{HCl} \cdot 1.8\text{H}_2\text{O}$: C, 52.34; H, 5.31; N, 19.42. Found: C, 52.50; H, 5.30; N, 19.25.

■ ASSOCIATED CONTENT

Ⓢ Supporting Information

Thermal profiles for the new heterocyclic cations, CD spectra for 17a, and ^1H and ^{13}C NMR spectra for the new intermediates and heterocyclic cations. This material is available free of charge via the Internet at <http://pubs.acs.org>.

■ AUTHOR INFORMATION

Corresponding Authors

*E-mail: wdw@gsu.edu.

*E-mail: dboykin@gsu.edu.

Notes

The authors declare no competing financial interest.

■ ACKNOWLEDGMENTS

This work was supported by the National Institutes of Health (Grant No. AI064200).

■ REFERENCES

- (1) Koehler, A. N. *Curr. Opin. Chem. Biol.* **2010**, *14*, 331–340.
- (2) Tidwell, R. R.; Boykin, D. W. In *Demeunynck, M., Bailly, C., Wilson, W. D., Eds. DNA and RNA Binders: From Small Molecules to Drugs*; Wiley-VCH: Weinheim, 2003; Vol. 2, pp 414–460.
- (3) Sharma, S. K.; Tandon, M.; Lown, J. W. *J. Org. Chem.* **2000**, *65*, 1102–1107.
- (4) Wilson, W. D.; Tanius, F. A.; Mathis, A.; Tevis, D.; Hall, J. E.; Boykin, D. W. *Biochimie* **2008**, *90*, 999–1014.
- (5) Suckling, C. *Future Med. Chem.* **2012**, *4*, 971–989.
- (6) Pandian, G. N.; Shinohara, K.; Ohtsuki, A.; Nakano, Y.; Masafumi, M.; Bando, T.; Nagase, H.; Yamada, Y.; Watanabe, A.; Terada, N.; Sato, S.; Morinaga, H.; Sugiyama, H. *ChemBioChem* **2011**, *12*, 2822–2828.
- (7) Yasuda, A.; Noguchi, K.; Minoshima, M.; Kashiwazaki, G.; Kanda, T.; Katayama, K.; Mitsuhashi, J.; Bando, T.; Sugiyama, H.; Sugimoto, Y. *Cancer Sci.* **2011**, *102*, 2221–2230.
- (8) Li, B.; Montgomery, D. C.; Puckett, J. W.; Dervan, P. B. *J. Org. Chem.* **2013**, *78*, 124–133.
- (9) Yang, F.; Nickols, N. G.; Li, B. C.; Marinov, G. K.; Said, J. W.; Dervan, P. B. *Proc. Natl. Acad. Sci. U.S.A.* **2013**, *110*, 1863–1868.
- (10) Edwards, T. G.; Koeller, K. J.; Slomczynska, U.; Fok, K.; Helmus, M.; Bashkin, J. K.; Fisher, C. *Antiviral Res.* **2011**, *91*, 177–186.
- (11) Benson, D. A.; Cavanaugh, M.; Clark, K.; Karsch-Mizrachi, I.; Lipman, D. J.; Ostell, J.; Sayers, E. W. *Nucleic Acids Res.* **2013**, *41*, D36–42.
- (12) Bishop, E. P.; Rohs, R.; Parker, S. C.; West, S. M.; Liu, P.; Mann, R. S.; Honig, B.; Tullius, T. D. *ACS Chem. Biol.* **2011**, *6*, 1314–1320.
- (13) Ecker, J. R.; Bickmore, W. A.; Barroso, I.; Pritchard, J. K.; Gilad, Y.; Seqal, E. *Nature* **2012**, *489*, 52–55.
- (14) Munde, M.; Wang, S.; Kumar, A.; Stephens, C. E.; Farahat, A. A.; Boykin, D. W.; Wilson, W. D.; Poon, G. M. *Nucleic Acids Res.* **2013**, DOI: 10.1093/nar/gkt955.
- (15) Nanjunda, R.; Wilson, W. D. *Curr. Protoc. Nucleic Acid Chem.* **2012**, *51*, 8.8.1–8.8.20.
- (16) Thuita, J. K.; Wang, M. Z.; Kagira, J. M.; Denton, C. L.; Paine, M. F.; Mdachi, R. E.; Murilla, G. A.; Ching, S.; Boykin, D. W.; Tidwell, R. R.; Hall, J. E.; Brun, R. *PLoS Negl. Trop. Dis.* **2012**, *6*, e1734.
- (17) Paine, M. F.; Wang, M. Z.; Generaux, C. N.; Boykin, D. W.; Wilson, W. D.; De Koning, H. P.; Olson, C. A.; Pohlig, G.; Burri, C.; Brun, R.; Murilla, G. A.; Thuita, J. K.; Barrett, M. P. *Curr. Invest. Drugs* **2010**, *11*, 876–883.
- (18) Wenzler, T.; Boykin, D. W.; Ismail, M. A.; Hall, J. E.; Tidwell, R. R.; Brun, R. *Antimicrob. Agents Chemother.* **2009**, *53*, 4185–4192.
- (19) Liu, Y.; Chai, Y.; Kumar, A.; Tidwell, R. R.; Boykin, D. W.; Wilson, W. D. *J. Am. Chem. Soc.* **2012**, *134*, 5290–5299.
- (20) Rahimian, M.; Kumar, A.; Say, M.; Bakunov, S. A.; Boykin, D. W.; Tidwell, R. R.; Wilson, W. D. *Biochemistry* **2009**, *48*, 1573–1583.
- (21) Nguyen, B.; Neidle, S.; Wilson, W. D. *Acc. Chem. Res.* **2009**, *42*, 11–21.
- (22) Neidle, S. *Nat. Prod. Rep.* **2001**, *18*, 291–309.
- (23) Wei, D.; Wilson, W. D.; Neidle, S. *J. Am. Chem. Soc.* **2013**, *135*, 1369–1377.
- (24) Wang, S.; Nanjunda, R.; Aston, K.; Bashkin, J. K.; Wilson, W. D. *Biochemistry* **2012**, *51*, 9796–9806.
- (25) Rettig, M.; Germann, M. W.; Wang, S.; Wilson, W. D. *ChemBioChem* **2013**, *14*, 323–331.

- (26) Singh, M. P.; Joseph, T.; Kumar, S.; Bathini, Y.; Lown, J. W. *Chem. Res. Toxicol.* **1992**, *5*, 597–607.
- (27) Chenoweth, D. M.; Poposki, J. A.; Marques, M. A.; Dervan, P. B. *Bioorg. Med. Chem.* **2007**, *15*, 759–770.
- (28) Farahat, A. A.; Paliakov, E.; Kumar, A.; Barghash, A. E.; Goda, F. E.; Eisa, H. M.; Wenzler, T.; Brun, R.; Liu, Y.; Wilson, W. D.; Boykin, D. W. *Bioorg. Med. Chem.* **2011**, *19*, 2156–2167.
- (29) Ramadas, K.; Srinivasan, N. *Synth. Commun.* **1992**, *22*, 3189–3195.
- (30) Wagner, G.; Horn, H. *Pharmazie* **1975**, *30*, 353–357.
- (31) Renneberg, D.; Dervan, P. B. *J. Am. Chem. Soc.* **2003**, *125*, 5707–5716.
- (32) Huel, N. H.; Nar, H.; Priepke, H.; Ries, U.; Stassen, J. M.; Wiene, W. *J. Med. Chem.* **2002**, *45*, 1757–1766.
- (33) Frutos, R. P.; Wei, X. D.; Patel, N. D.; Tampone, T. G.; Mulder, J. A.; Busacca, C. A.; Senanayake, C. H. *J. Org. Chem.* **2013**, *78*, 5800–5803.
- (34) Boykin, D. W.; Kumar, A.; Spychala, J.; Zhou, M.; Lombardy, R. J.; Wilson, W. D.; Dykstra, C. C.; Jones, S. K.; Hall, J. E.; Tidwell, R. R.; Laughton, C.; Nunn, C. M.; Neidle, S. *J. Med. Chem.* **1995**, *38*, 912–916.
- (35) Pinner, A.; Klein, F. *Ber. Dtsch. Chem. Ges.* **1877**, *10*, 1889–1897.
- (36) Ismail, M. A.; Batista-Parra, A.; Miao, Y.; Wilson, W. D.; Brun, R.; Wenzler, T.; Boykin, D. W. *Bioorg. Med. Chem.* **2005**, *13*, 6718–6726.
- (37) Oguchi, M.; Wada, K.; Honma, H.; Tanaka, A.; Kaneko, T.; Sakakibara, S.; Ohsumi, J.; Serizawa, N.; Fujiwara, T.; Horikoshi, H.; Fujita, T. *J. Med. Chem.* **2000**, *43*, 3052–3066.
- (38) Miyaura, N.; Suzuki, A. *Chem. Rev.* **1995**, *95*, 2457–2483.
- (39) Ismail, M. A.; Boykin, D. W. *Synth. Commun.* **2011**, *41*, 319–330.
- (40) Wilson, W. D.; Tanius, F. A.; Fernandez-Saiz, M.; Rigl, C. T. *Methods Mol. Biol.* **1997**, *90*, 219–240.
- (41) Rettig, M.; Kamal, A.; Ramu, R.; Mikolajczak, J.; Weisz, K. *Bioorg. Med. Chem.* **2009**, *17*, 919–928.
- (42) Shi, X. C.; Chaires, J. B. *Nucleic Acids Res.* **2006**, *34*, e14.
- (43) Hancock, S. P.; Ghane, T.; Cascio, D.; Rohs, R.; Felice, R. D.; Johnson, R. C. *Nucleic Acids Res.* **2013**, *41*, 6750–6760.
- (44) Rohs, R. S.; West, E.; Sosinsky, A.; Liu, P.; Mann, R. S.; Honig, B. *Nature* **2009**, *461*, 1248–1253.
- (45) Norden, B.; Kubista, M.; Kurucsev, T. *Q. Rev. Biophys.* **1992**, *25*, 51–170.
- (46) Seidel, C. A. M.; Schulz, A.; Sauer, M. H. M. *J. Phys. Chem.* **1996**, *100*, 5541–5553.
- (47) Edman, L.; Mets, U.; Rigler, R. *Proc. Natl. Acad. Sci. U.S.A.* **1996**, *93*, 6710–6715.
- (48) Neubauer, H.; Gaiko, N.; Berger, S.; Schaffer, J.; Eggeling, C.; Tuma, J.; Verdier, L.; Seidel, C. A. M.; Griesinger, C.; Volkmer, A. *J. Am. Chem. Soc.* **2007**, *129*, 12746–12755.
- (49) Nguyen, B.; Tanius, F. A.; Wilson, W. D. *Methods* **2007**, *42*, 150–161.
- (50) Liu, Y.; Wilson, W. D. *Methods Mol. Biol.* **2012**, *613*, 1–23.
- (51) Nanjunda, R.; Munde, M.; Liu, Y.; Wilson, W. D. In *Methods for Studying DNA/Drug Interactions*; Wanunu, M., Tor, Y., Eds.; CRC Press-Taylor & Francis Group: Boca Raton, FL, 2011; Chapter 4.
- (52) Minehan, T. G.; Gottwald, K.; Dervan, P. B. *Helv. Chim. Acta* **2000**, *83*, 2197–2213.
- (53) Viger, A.; Dervan, P. B. *Bioorg. Med. Chem.* **2006**, *14*, 8539–8549.
- (54) SYBYL Molecular Modeling Software, Version X1.2, Tripos Inc.: St. Louis, MO, 2010.
- (55) Liu, Y.; Collar, C. J.; Kumar, A.; Stephens, C. E.; Boykin, D. W.; Wilson, W. D. *J. Phys. Chem. B* **2008**, *112*, 11809–11818.
- (56) Collar, C. J.; Lee, M.; Wilson, W. D. *J. Chem. Inf. Model* **2010**, *50*, 1611–1622.